NASA CR-62039

INSTITUTE FOR DIRECT ENERGY CONVERSION

TOWNE SCHOOL

UNIVERSITY OF PENNSYLVANIA

PHILADELPHIA, PENNSYLVANIA

MANFRED ALTMAN, DIRECTOR

STATUS REPORT

INDEC-SR-9

GRANT NSG - 316

October 31, 1966

NATIONAL AERONAUTICS AND SPACE ADMINISTRATION

For sale by the Clearinghouse for Federal Scientific and Technical Information
Springfield, Virginia 22151 – CFSTI price $3.00

TABLE OF CONTENTS

LIST OF ILLUSTRATIONS

1. INTRODUCTION AND SUMMARY

1. Introduction and Summary

The Institute for Direct Energy Conversion has passed its formative period, and is a "going concern."

In addition to the research work reported here, the support which we have received from NASA has also had the following beneficial effects.

Nine students have obtained their doctorates under the auspices of the Institute. Two more are expected to obtain their degrees in 1966.

The Institute is currently supporting the work of twelve faculty members and seventeen graduate students.

The Energy Conversion courses which were generated have found good acceptance by the students. Twenty-five students are presently enrolled in Direct Energy Conversion courses.

To date, thirty-six papers have been published, and most of these were accepted by "prestige" journals.

Three patent applications have been filed, and were transmitted to NASA.

At present the Institute has more applications for support than it can accommodate.

The overall effect of our program on the University of Pennsylvania has been a gratifying one, as measured by faculty and student participation.

A significant development has been the generation of multi-disciplinary research projects, which could only have been conceived in an atmosphere of the type which the Institute provides.

2. MATERIALS ENGINEERING

Branch Chief: Dr. Solomon Pollack

Senior Members: Dr. Manfred Altman, Dr. Louis Girifalco, Dr. Ram Sharma

2.1 High Temperature Thermal Diffusivity Measurements

Senior Investigators: Dr. Manfred Altman, Dr. Ram Sharma

Ph.D. Students: H. Keramaty, E. Hopfinger, K. Sreenivasan

Objectives

Phase 1. To develop an experimental technique suitable for the determination of thermal diffusivities at temperatures up to 2000°C, primarily for the testing of thermal energy storage compounds in the solid state.

Phase 2. To extend the technique to the study of liquids.

Phase 3. To apply the technique to the study of physical mixtures of different compounds.

Previous Accomplishments

Phase 1.

1. A transient technique was developed with the following desirable characteristics:

   a. Only temperature measurements need be made. (no heat balance requirements)

   b. Solids can be studied right up to the melting point.

   c. Rapid results can be obtained.

2. First results of this work have been accepted for presentation at the 1966 A.S.M.E. Winter Annual Meeting, and for publication by the A.S.M.E. Journal.

3. A Ph.D. degree was granted to H. Chang for satisfactory completion of this work.

Phase 2. Analytical results had shown that the study of liquids in the apparatus was feasible. Specifically it was shown that the obtainable

resolution was acceptable. It was reported that the apparatus would be made available to N.A.S.A. if such a need existed.

Phase 3. Mixture samples were being made.

Progress in Past Period

1. CaF_2, BaF_2, and (66.7% BaF_2-CaF_2) samples were made. Densities were measured and compared to theoretical values. Good agreement was obtained.

2. Thermal diffusivity measurements were made of the pure compounds. Testing of the mixture sample is in progress.

Details are presented on page A2-1 of this report.

2.2 Thermoelectric Properties of Graphite Compounds

Senior Investigators: Dr. L. Girifalco, Dr. S. Pollack

Graduate Students: T. DiVincenzo, T. Montelbono, S. Sachidanandam

Objectives

The objective of this work is to determine the feasibility of synthesizing a new class of thermoelectric compounds which would have superior thermoelectric properties. It is believed that the introduction of metallic impurities into a graphite crystal will result in a broadening of the band gap and will, at the same time, decrease phonon conduction without effecting electronic conduction. At the present time, theoretical studies are in progress which will result in the prediction of obtainable band gaps and the prediction of achievable electron transport by the hopping mechanism. It is planned to use the results of this theoretical work in the fabrication of such new materials and to determine their thermoelectric properties experimentally.

Previous Accomplishments

The modified Kronig-Penny model has yielded preliminary results showing electron effective mass as a function of potential well depth. Barium has been diffused into graphite, and X-ray studies are in progress. Equipment has been constructed to measure thermoelectric power as a function of temperature from $77^{\circ}K$ to $400^{\circ}K$.

Progress in Past Period

A modified Kronig-Penny model was suggested. Equipment partially designed for TEP measurements.

2.3 Tunnel Emission Cold Cathodes

Senior Investigator: Dr. S. Pollack
Graduate Student: S. Basavaiah

Objectives

The purpose of this investigation is to develop efficient cold cathodes for electric devices, and, eventually to the development of tunnel emission devices and the study of hot electron transport phenomena. The by-products of this work are expected to be a better understanding of the electron scattering mechanisms in thin films with applicability to thin film solar cells and similar devices.

Previous Accomplishments

A new vacuum system was designed and fabricated to obviate the problems introduced by the Elion system.

Progress in Past Period

Electron beam evaporation of W was tried in Elion system and, due to poor design of cryopump and sublimation pump, the pressure rise during heating was excessive. Evaporation could not be accomplished. For details see Page A2-8.

2.4 Studies of Thermal Transpiration for the Development of a "Thermal Pump"

Dr. M. Altman, Mr. E. Hopfinger

Objectives

To develop a gas (or vapor) pump without moving parts, based on the thermal transpiration principle.

Previous Accomplishments

New project.

Progress in Past Period

Theoretical analyses were made, and preliminary design experiments were performed. Equipment is being assembled. Details on page A2-10.

3. PLASMA ENGINEERING

Branch Chief: George L. Schrenk

Senior Members: Maurice A. Brull, Chad F. Gottschlich
Michael Kaplit, Samuel Schweitzer
Hsuan Yeh, Leon W. Zelby

3.1 Characteristics of Plasma Probes in a MHD Working Fluid

Hsuan Yeh, A. Whitman

Objectives

To extend the theory of probes to cases including recombination effects and the sheath.

Previous Accomplishments

An analytical investigation of the sheath region has been made and range of validity into separating the entire region into a collision dominated one, and a free field zone has been made. Closed form solutions for several important cases have been found. Present work is concerned with an experimental study which utilizes probes which are biased with kilocycle frequencies. The results of this work to date will be presented at the 1966 International MHD Meeting.

Progress in Past Period

Work completed (see INDEC SR-8) and Whitman Dissertation.

3.2 Slow Waves as a Plasma Diagnostic Tool

Leon W. Zelby, W. O. Mehuron, R. J. Kalagher

Objectives

To develop slow wave plasma interaction for measurement of local plasma parameters.

Previous Accomplishments

Mathematical model was developed which relates measurements of insertion loss, phase shifts and Doppler shift to the local values of electron number density, electron-neutral molecule collision frequency, and electron drift velocity. From these measurements, it is possible to deduce the percentage of ionization, electron temperature, and conductivity. See also W. O. Mehuron dissertation and R. J. Kalagher dissertation.

Progress in Past Period

Previous model was extended to include variations of collision frequency. For details see Page A3-1.

3.3 Measurement of Plasma Transport Properties in a Na-K Seeded Argon Plasma

Chad F. Gottschlich, T. K. Chu

Objectives

Measurement of the non-equilibrium ionization which is produced by an externally applied electric field in a sodium-potassium seeded argon plasma.

Previous Accomplishments

The major result was the demonstration that the plasma is remarkably uniform except for a very small region in the neighborhood of the confining wall. It was also shown that not only are increased electron temperatures obtained, but the temperature of the bulk plasma itself increases significantly over its equilibrium value.

Progress in Past Period

Work completed (see T. K. Chu dissertation).

3.4 Transport Properties of Partially Ionized Gases

Samuel Schweitzer

Objectives

To improve the accuracy of calculation of conductivities of ionized gases.

Previous Accomplishments

The results of this work have shown that existing methods of predicting the behavior of mixtures are not reliable and can sometimes over-estimate the electrical conductivity as much as 70%. Results of this work have been published in the Proceedings of the Sixth MHD Symposium, April 1965. Future research is concerned with extending the analytical technique to thermal conductivities.

Progress in Past Period

Conductivity calculations of ionized gas with about 20% accuracy were obtained. For details see Page A3-3.

3.5 Electron Emission from Metals in Gaseous Environment

M. Kaplit, L. Zelby, G. Schrenk

Objectives

To refine the calculation of electron emission from metals in gaseous environment.

Previous Accomplishments

The Thomas-Fermi-Dirac theory has been used to evaluate the microscopic charge distribution and the total energy of metal plasma interface. Results of this work show that quantum mechanical corrections are a significant part of the total energy and may not be neglected. A quantum-chemical microscopic model of electron emission for metals in gaseous environments has been developed. Electron emission S curves have been calculated for cesium-tungsten and cesium-fluorine.

Progress in Past Period

Work completed (see INDEC SR-8 and Publication List).

3.5.1 The Influence of High Fields on Surface Charge Distributions

G. L. Schrenk, S. Fonash

Objectives

To determine the effect of high fields on the work function of metals.

Previous Accomplishments

Research initiated.

Progress in Past Period

Preliminary work on a computer model is in progress.

For details see Page A3-4.

3.5.2 Anisotropy of Metal Work Functions

M. Kaplit

Objectives

To develop a model accounting for different results of measurements of the work function of tungsten.

Previous Accomplishments

Mathematical model was developed, and results given in INDEC SR-8.

Progress in Past Period

Effects of surface stresses and polarizabilities were calculated.

For details see Page A3-5.

3.6 Characteristics of Thermionic Plasma Diodes with Gas Mixtures

George L. Schrenk, Allen Kaufman

Objectives

To develop a quantitative model for "seeded" diodes for the purpose of evaluating the Penning effect.

Previous Accomplishments

Mathematical model for the determination of ionization rate was developed.

Progress in Past Period

The mode was extended to include ignited and unignited modes.

For details see Page A3-8.

3.7 Plasma Centrifuge

M. Altman S. Schweitzer

P. Hsueh

Objectives

To evaluate obtainable velocities in a plasma spinning in the annular space between two concentric cylinders under the influence of a longitudinal magnetic field and a radial electric field.

Previous Accomplishments

Theoretical analysis for the case of liquid mercury was completed (for details see INDEC SR-8).

Progress in Past Period

Results in the case of small magnetic Reynolds number, and negligible Hall effect were obtained. (for details see INDEC SR-8 and Page A3-9.

4. ELECTROCHEMICAL ENGINEERING

Branch Chief: Dr. Leonard Nanis

Senior Member: Dr. John O'M. Bockris

Postdoctoral Research Associate: Dr. Philippe Javet

4.1 Atomic Scale Electrode Processes

Dr. Philippe Javet, Dr. L. Nanis

Objectives

Field-ion emission microscope studies - the objectives of this work are to develop techniques for the use of the field-ion microscope to allow the determination of the electrochemical adsorption of oxygen onto noble metals used as fuel cell catalysts. The successful development of this technique will make it possible to obtain a visualization of the result of motion of atoms and ionic species on metal electrodes and across the interface between electrode and electrolyte.

Previous Accomplishments

A commercial model (Central Scientific Company) field-ion emission microscope (FIM) has been installed and put into operation.

Progress in Past Period

Tungsten tips have been used to check out FIM performance. Steps are being taken to improve the resolution of platinum tips. For details see Page A4-1.

4.2 Freezing Potentials

Dr. L. Nanis, Mr. Irving Klein

Objectives

Freezing potentials (Workman-Reynolds effect) result from a complex interplay of factors such as adsorption of ions, rate of ice growth, and solution concentration. The phenomenon of charge separation must ultimately bear a relationship to electrode interfacial capacitance and double layer structure. A systematic study is to be made of various surface conditions to tie in the electrochemistry of this phenomenon. Possible applications exist in the areas of water purification and cloud electrification.

Previous Accomplishments

Equipment for monitoring freezing potentials and temperature variation has been designed, constructed, and tested. Previously known concentration effects were verified, i.e. the sign of the potential depends on the nature of dilute ionic species and the effect diminishes at very low ($< 10^{-6}$M) and very large ($>10^{-3}$M) concentrations.

Progress in Past Period

1. A definite effect of the nature of the substrate on the freezing potential has been found, suggesting an orienting effect of water adsorbed in the double layer on the ice-liquid interface during subsequent growth.

2. A definite relation between freezing time and potential has been observed. For any given solution on the various substrates, a maximum potential is attained at a definite freezing time. This effect is also related to the substrate effect, indicating that the rate of ice formation depends on the electrochemical nature of the initial solution-metal interface. Such an effect is hitherto unreported. For details see Page A4-4.

4.3 Oxidation of Hydrogen on Platinum Electrodes

Dr. L. Nanis , Mr. George Rowell

Objectives

To study meniscus heating in a porous electrode model and to determine gross surface effects caused by oxygen absorbed on platinum in a hydrogen saturated electrolyte.

Accomplishments to Date

Pore geometry was approximated with a vertical sheet of 1 N H_2SO_4 in contact with a smooth platinum electrode. Anodic polarization for six minutes at a potential of + 1.5 volts (N.H.E.) was chosen as a standard initial treatment. An experimental sequence involving exposure to hydrogen gas at various times during the decay of potential following current interruption were worked out. The meniscus heating effect was found to be negligible (less than $0.01^{\circ}C$) on the scale studied (0.5mm).

Accomplishment of Latest Period

1) Definite evidence was obtained for a distinct change in wetting behavior of the platinum at a potential of + 0.74 V. A thin film of electrolyte adheres to platinum which has been polarized to + 1.5V. The film of electrolyte drains rapidly and leaves residual beads when potential is less than 0.74V. The consequences of this behavior are important regarding porous electrode flooding in fuel cell operation and also in terms of models of the surface oxides on platinum. For details see Page A4-8.

4.4 Concentration Overpotential Transients

Dr. L. Nanis, Mr. A. Adubifa

Objectives

To develop analysis of concentration overpotential transients to provide a new means for measuring the mass transport boundary layer in electrochemical systems.

Accomplishments to Date

Vertical silver anodes in 0.1M $AgNo_3$ solution were studied over a wide range of current density. Build-up and decay transients were obtained.

Accomplishment of Last Period

All results for build up of overpotential were analyzed and error limits established. Comparison of boundary layer thickness evaluated from these results shows excellent agreement with theoretical calculations based on the hydrodynamics of natural convection flow.

For details see Page A4-12.

4.5 Galvanostatic Charging Transients

Dr. L. Nanis, Dr. P. Javet

Objectives

To develop a simple and practical mathematical treatment for the time variation of activation overpotential following a **step** in current.

Accomplishments to Date

None, new project.

Accomplishment in Last Period

A simplified rate expression was developed which, although an approximation, contains the feature of zero overpotential at zero current (in contrast with the Tafel approximation). For constant interfacial capacitance, a form is obtained which is easily integrated giving time as a function of overpotential in a simple mathematical form. It appears possible to treat various transfer coefficients and also potential dependent capacitance in a relatively straightforward analytical fashion. For details see Page A4-17.

5. PH.D'S GRANTED

Ph.D's Granted

M. Kaplit: Ph.D. Dissertation, The Surface Double Layer of a Metal Work Function in a Gaseous Environment.

Y. K. Rao: Ph.D. Dissertation, Thermodynamic Properties of Binary Liquid Magnesium Solutions.

Frederic Costello: Ph.D. Dissertation, Optimization of Large Systems with Non-Linear Heat Transfer Phenomena.

Daniel P. Ross: Ph.D. Dissertation, Droplet Formation and Vaporization in the Wake of a Melting Body.

Han Chang: Ph.D. Dissertation, An Unsteady-State Technique to Measure Thermal Diffusivity of High Temperature Materials.

William Mehuron: Ph.D. Dissertation, Electromagnetic Wave Interaction in an Inhomogeneous Drifting Plasma.

Alan Whitman: Ph.D. Dissertation, Theory of Electrostatic Probes in a Magnetohydrodynamic Fluid.

T. K. Chu: Ph.D. Dissertation, Temperature Measurement of an Alkali Metal-Seeded Plasma in an Electric Field.

Richard Kalagher: Ph.D. Dissertation, Determination of Electron Density and Collision Frequency in a Cylindrical Plasma Column by the Use of Slow Waves.

6. PUBLICATIONS LIST

Publications List

INDEC-1 H. Yeh and T. K. Chu, "The Optimization of MHD Generators with Arbitrary Conductivity," ASME Paper 63-WA-349.

INDEC-2 M. Altman, D. P. Ross, H. Chang, "The Prediction of Transient Heat Transfer Performance of Thermal Energy Storage Devices, Proceedings of 6th National Heat Transfer Conference, Boston, Mass., 1963.

INDEC-3 G. R. Belton and Y. K. Rao, "The Binary Eutectic as a Thermal Energy Storage System: Equilibrium Properties," paper presented at the 6th National Heat Transfer Conference, Boston, Mass. Aug. 11-14, 1963.

INDEC-4 J. Dunlop and G. Schrenk, "Theoretical Model of a Thermionic Converter," Proceedings of Thermionic Specialist Conference, Gatlinburg, Tenn., pp. 57-62, Oct. 7-9, 1963.

INDEC-5 R. Sharma and H. Chang, "Thermophysical and Transport Properties of High Temperature Energy Storage Materials," paper presented at the Third Annual Symposium, High Temperature Conversion Heat to Electricity, Tucson, Arizona, Feb. 19-21, 1964.

INDEC-6 G. L. Schrenk, "Solar Collection Limitations for Dynamic Converters-Simulation of Solar-Thermal Energy Conversion Systems," Proceedings of AGARD Conference, Cannes, France, March 16-20, 1964.

INDEC-7 M. Altman, "Prospects for Thermal Energy Storage," Proceedings of AGARD Conference, Cannes, France, March 16-20, 1964.

INDEC-8 L. Zelby, "The Hollow Thermionic Converter," IEEE Annual Meeting on Energy Conversion, Clearwater, Florida, May 1964.

INDEC-9 M. Altman, "The Institute for Direct Energy Conversion," paper presented at Am. Soc. Eng. Ed. Annual Meeting, University of Maine, Orono, Maine, June 22-26, 1964.

INDEC-10 G. Schrenk, "Emitter Sheath Polarity in Plasma Diodes, Proceedings of Thermionic Specialist Conference, Cleveland, Ohio, Oct. 26-28, 1964, pp. 249-257.

INDEC-11 M. Kaplit, G. Schrenk, L. Zelby, "Electron Emission from Metals in Gaseous Environment," Proceedings of Thermionic Specialist Conference, Cleveland, Ohio, Oct. 26-28, 1964, pp. 4-10.

INDEC-12 G. Schrenk, "Criteria for Emitter Sheath Polarity in Plasma Diodes," paper presented at ASME Winter Annual Meeting, New York, No. 29, Dec. 3, 1964.

INDEC-13 R. J. Blasco and E. Gileadi, "An Electrochemical and Microbiological Study of the Formic Acid-Formic Dehydrogenlyase System," Advanced Energy Conversion, Vol. 4, pp. 179-186, 1964.

INDEC-14 G. Schrenk and A. Lowi, "Mathematical Simulation of Solar Thermionic Energy Conversion Systems," Proceedings of the International Thermionic Electrical Power Generation Conference, IEEE, London, England, Sept. 20-24, 1965.

INDEC-15 R. McKinnon, A. Turrin, G. Schrenk, "Cavity Receiver Temperature Analysis," AIAA paper No. 65-470, July 26-29, 1965.

INDEC-16 G. Schrenk and M. Kaplit, "Electron Emission from Metals in Vapors of Cesium and Fluorine," Proceedings of the Thermionic Specialist Conference, San Diego, California, Oct. 25-27, 1965.

INDEC-17 C. A. Renton and L. W. Zelby, "Longitudinal Interaction of Microwaves with an Argon Discharge," Appl. Phys. Ltrs., Vol. 6, No. 8, pp. 167-169, Sept. 15, 1965.

INDEC-18 L. W. Zelby, "Microwave Interaction with a Non-Uniform Argon Discharge," Proceedings of the Symposium of Microwave Interaction with Ferrimagnetics and Plasmas, London, England, pp. 32-1 to 32-3, Sept. 13-17, 1965.

INDEC-19 M. Altman and J. H. Jones, "Two-Phase Flow and Heat Transfer for Boiling Liquid Nitrogen in Horizontal Tubes," Chemical Engineering Progress Symposium Series, Volume 61, No. 57, Oct. 1965.

INDEC-20 S. Schweitzer and M. Mitchner, "Electrical Conductivity of a Partially Ionized Gas in a Magnetic Field," Submitted to the AIAA Journal.

INDEC-21 M. Kaplit and G. L. Schrenk, "Models for Electron Emission from Metals with Adsorbed Monolayers," submitted to Advanced Energy Conversion.

INDEC-22 M. Kaplit and G. L. Schrenk, "Models for Electron Emission from Metals with Adsorbed Monolayers," paper presented at Twenty-Sixth Annual Conference on Physical Electronics,

Massachusetts Institute of Technology, Cambridge, Mass., March 21-23, 1966.

INDEC-23 L. W. Zelby, "Slow Wave Interaction with an Argon Discharge," (Abstract) Symposium on Properties and Applications of Low-Temperature Plasmas, XX-th International Congress of I.V.P.A.C., Moscow, USSR, July 15-18, 1965.

INDEC-24 L. W. Zelby, "Understanding Plasma Diodes and Amplifiers," Electronic Industries, Vol. 24, No. 11, p. 64, Nov. 1965.

INDEC-25 L. W. Zelby, "A Simplified Approach to the Analysis of Electromagnetic Wave Propagation Characteristics of Plasma Coated Surfaces," RCA Review, Vol. 26, No. 4, p. 497, Dec. 1965.

INDEC-26 L. W. Zelby, "Plasma Coated Surface as a Wave Guide" RCA Engineer, Vol. 11, No. 4, p. 50, Jan. 19, 1966

INDEC-27 L. W. Zelby, W. O. Mehuron, R. Kalagher, "Measurements of Collision Frequency in an Argon Discharge", Applied Physics Letters, Vol. 21, No. 5, June 1966.

INDEC-28 R. Kalagher, "Effects of Inhomogeneous Electron Density in a Cylindrical Plasma Column Surrounded by a Helix", submitted to IEEE Transactions on Microwave Theory and Techniques, March 1966.

INDEC-29 Samuel Greenhalgh, "Syringe for Injecting Sodium Potassium Alloy", submitted to The Review of Scientific Instruments, August 13, 1965.

INDEC-30 A. Whitman, H. Yeh, "Characteristics of Plasma Probes in a MHD Working Fluid", to be presented at International Symposium on Magnetohydrodynamic Electrical Power, Salzburg, Austria.

INDEC-31 S. Schweitzer, M. Mitchner, "Convergence of Successive Approximations to the Scalar Electrical Conductivity of Some Weakly Ionized Real Gases", to be published in the A.I.A.A. Journal.

INDEC-32 "The Determination of Thermal Diffusivities of Thermal Energy Storage Materials, Part 1, Solids Up To Melting Point", Han Chang, Manfred Altman, Ram Sharma. Accepted for publication in the A.S.M.E. Journal.

INDEC-33 "Electrochemical Principles of Corrosion", Leonard Nanis, to be given at National Association of Corrosion Engineers Symposium, September, 1966, Philadelphia, Pa.

INDEC-34 "Tolerance Specification by Multiple Alignment Statistics", L. Nanis, to be given at session "Effective Utilization of Grid-Based Interconnection Systems", 1966 Western Electronic Show and Convention, Los Angeles, California.

INDEC-35 "On the Tensor Electrical Conductivity of Atmospheric Cesium-Seeded Argon", S. Schweitzer, submitted to the A.I.A.A. Journal.

INDEC-36 "The Reaction of Molten Metal Droplets with a Rarefield Atmosphere", by M. Altman, D. Ross. Accepted for publication in the A.I.A.A. Journal.

MATERIALS ENGINEERING

APPENDIX 2

Thermal Diffusivity

Dr. R. A. Sharma, Mr. H. Keramaty

Experiments have been conducted to measure thermal diffusivity of solid barium fluoride and calcium fluoride materials. The samples have been prepared by the technique described in earlier report. The density of the samples so prepared is given in Table I.

Table I

Samples	Density in literature	Density of the sample prepared
CaF_2	3.18	2.96
BaF_2	4.83	4.36
(CaF_2+BaF_2)	4.28 (calculated)	4.18

The table also contains the density of the BaF_2+CaF_2 mixture of the composition 66.7% BaF_2 at 33.3 % CaF_2. The density of the mixture sample agrees well with the calculated one.

The results of the thermal diffusivity measurements of CaF_2 and BaF_2 samples are given in Figures 1 and 2. Further work is in progress for thermal diffusivity measurements of the fluoride mixture samples.

Figure 1

Thermal Diffusivity of Calcium Fluoride (CaF_2) vs. Temperature

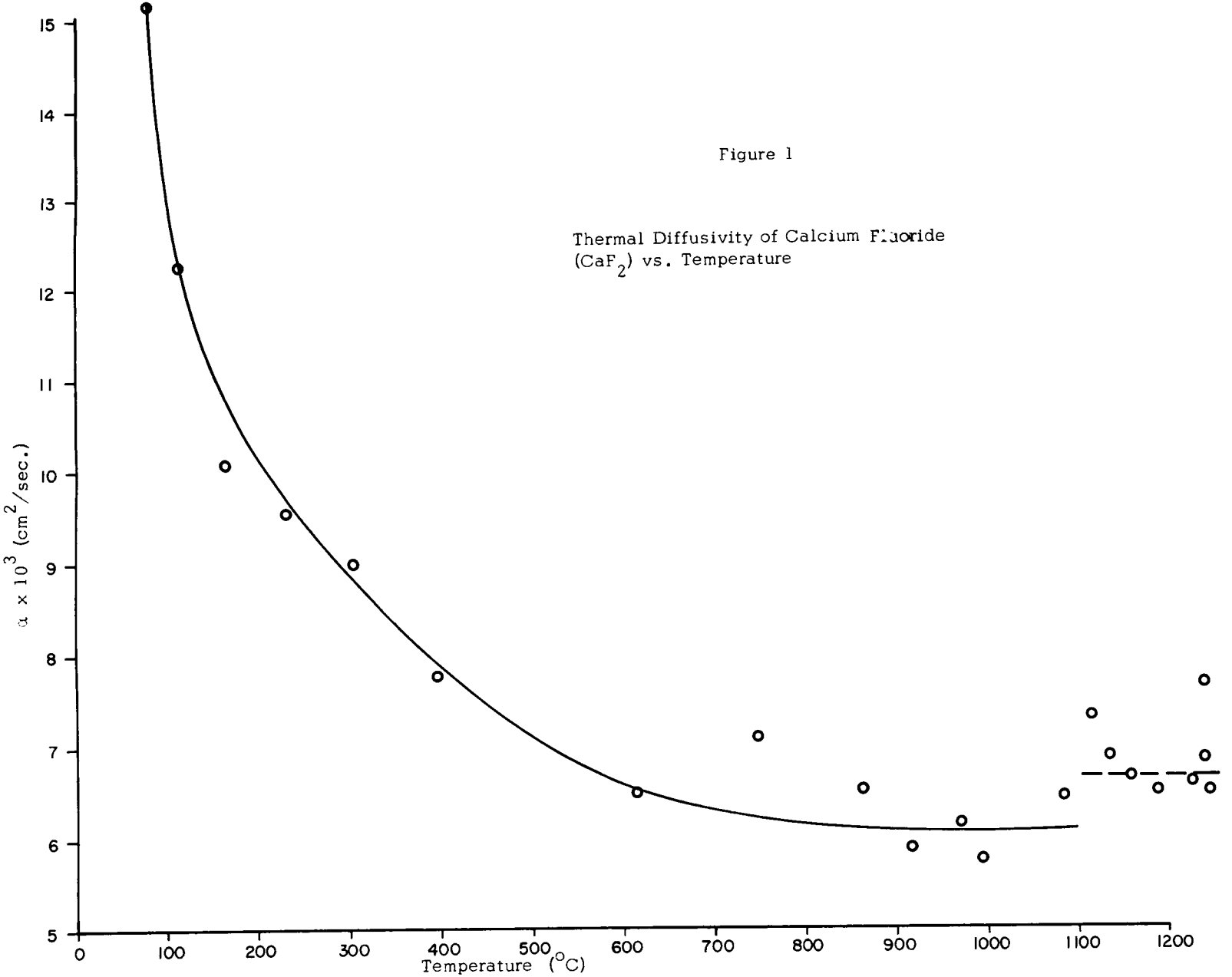

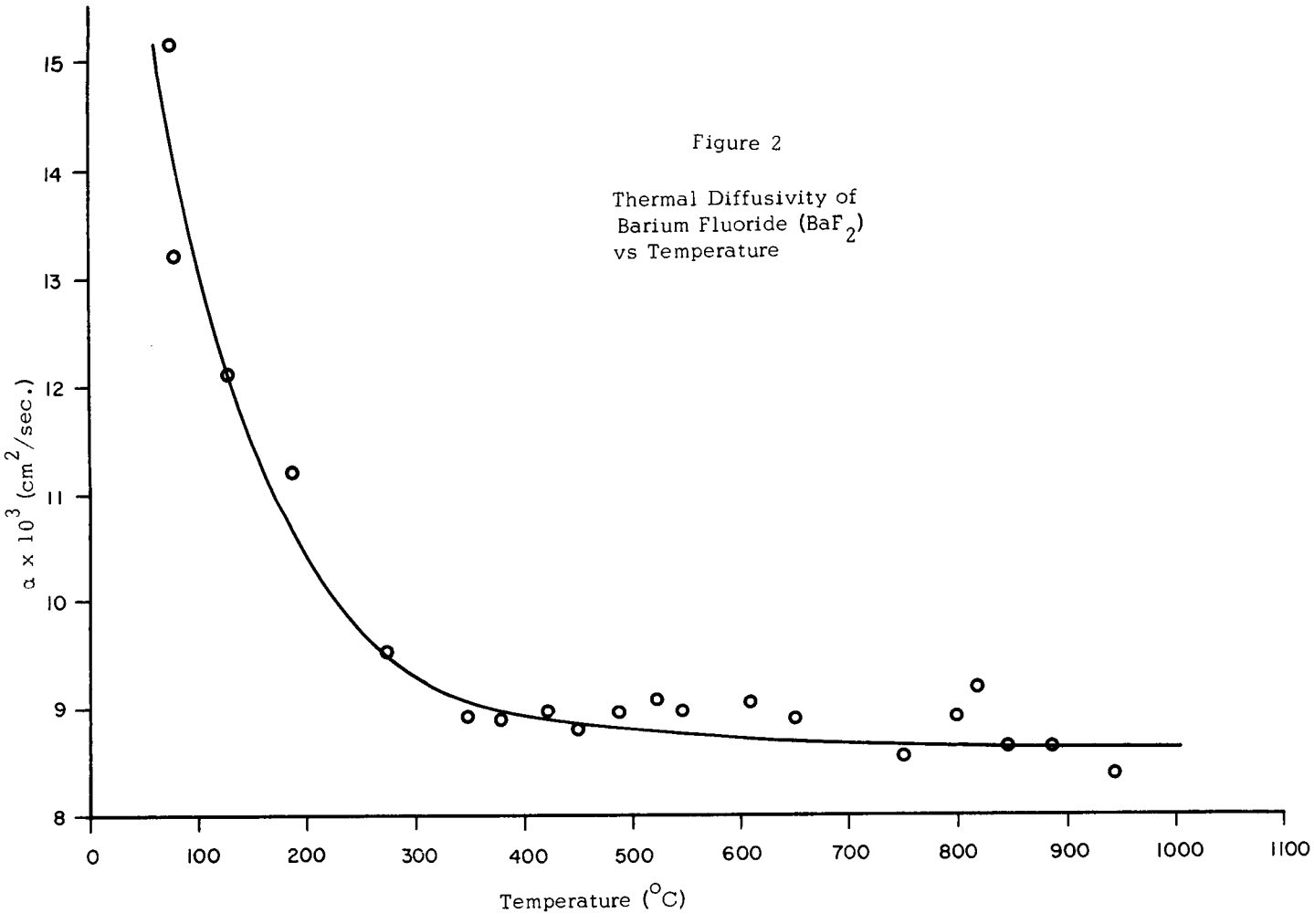

Figure 2

Thermal Diffusivity of
Barium Fluoride (BaF_2)
vs Temperature

Thermal Diffusivity of Liquids

Senior Investigators: Dr. Manfred Altman, Dr. Ram Sharma

Ph.D. Student: K. Sreenivasan

The theory and the experimental details of the method has been described in previous reports. Briefly, the method consists in raising linearly the surface temperature of a cylindrical container. The liquid, whose thermal diffusivity is to be measured, is introduced into an annular gap in the cylindrical container. The thermal diffusivity of the liquid is calculated by measuring the difference in temperature at the surface and at the center of the cylindrical container. No liquid temperature need be measured in this method.

The sensitivity of such a diffusivity cell can be taken to be the variation in the temperature difference for a given variation in the thermal diffusivity of the liquid. Analytical evaluation of the sensitivity is the subject of this report. The following are the relevant parameters used in the calculation. The expression for the temperature difference is given in Ref. 1.

Material of the cylindrical container - Boron Nitride

Annular gap width - 0.130 inch

Heating Rate - $1^{\circ}F$/Second

Outside diameter of the container - 2.04 inches

The sensitivity is shown graphically in Fig. 1.

A 2 1/2" diameter tubular furnace has been designed and built. Preliminary experiments to determine the thermal diffusivity of the container material have been completed. Liquid diffusivity measurements will soon be taken up.

References

1. "High Temperature Thermal Diffusivity Measurements", pp. 2-2 and 2-3, Status Report, INDEC-SR-8, Institute for Direct Energy Conversion, University of Pennsylvania.

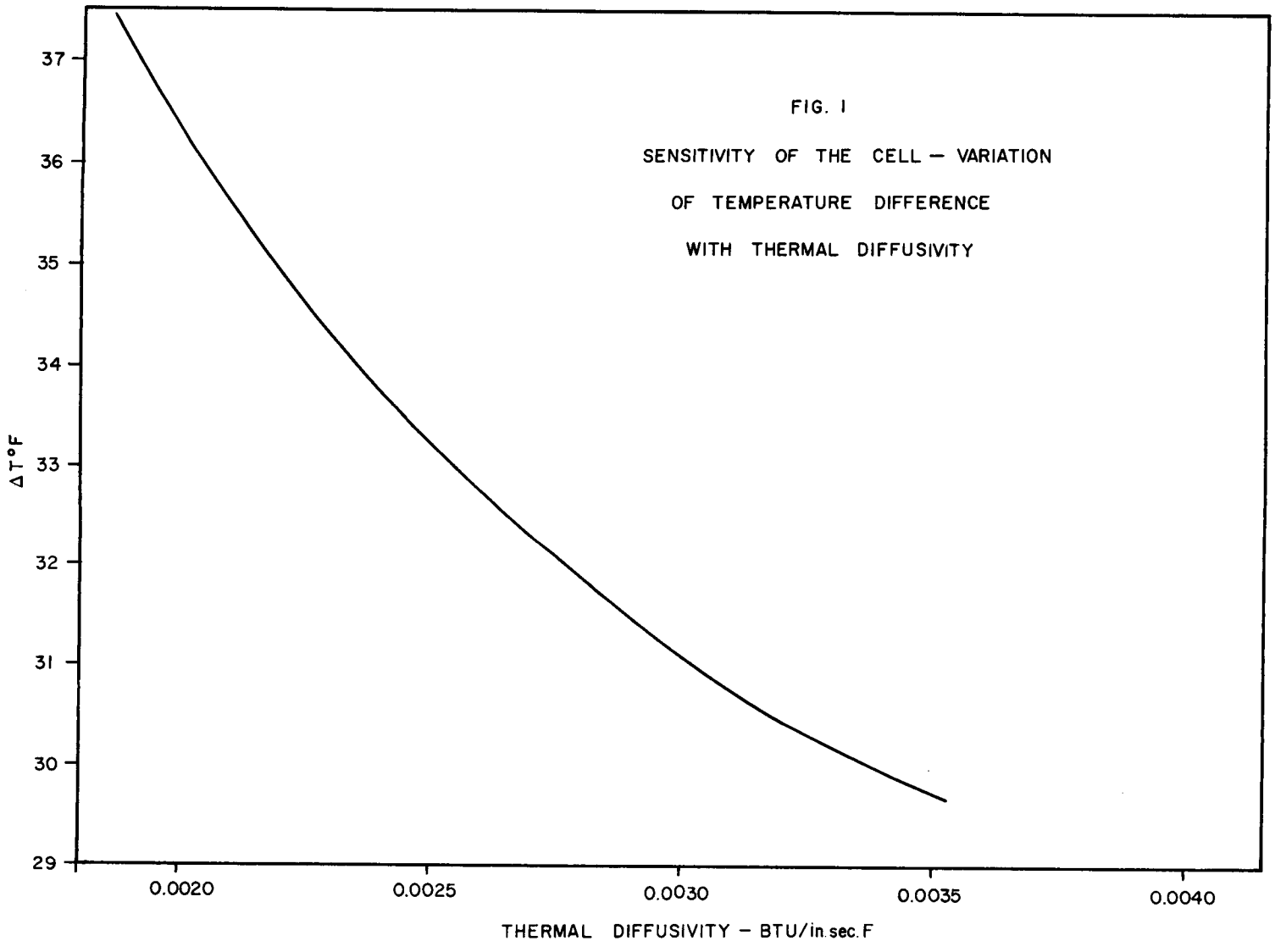

FIG. 1

SENSITIVITY OF THE CELL – VARIATION

OF TEMPERATURE DIFFERENCE

WITH THERMAL DIFFUSIVITY

Thermoelectric Properties of Graphite Compounds

Senior Investigators: Dr. L. Girifalco, Dr. S. Pollack

Graduate Students: T. DiVincenzo, T. Montelbono, S. Sachidanandam

I. Equipment Design and Construction

Construction of apparatus for measurement of electronic parameters is essentially complete. Consistent, reproducible results on standard samples (silver) have been obtained for thermoelectric power measurements.

II. Materials

Attempts to prepare graphite-tin alloys have been dropped for the time being because of several unsuccessful experiments. Attempts to prepare graphite-barium alloys seem to have been successful. A blue-black substance has been obtained by heating graphite and barium vapor. X-ray analysis indicates this substance is a lamellar compound. Further work is in progress to characterize the structure more completely and improve the method of preparation.

III. Theoretical

Work is being done on the extended Kronig-Penney model for the band structure of graphite outlined in the last report.

Effective masses in the C-direction have been computed for the first five bands as a function of the sheet potential. Harrison plots for graphite are being constructed in order to compare the free electron model to the Kronig-Penney and tight binding models.

A model for the thermal conductivity of graphite compounds has been constructed based on elementary heat transfer and phonon

transport theory. Calculations based on this model strongly suggest that the decrease of phonon conductivity to be expected on forming lamellar compounds of graphite is quite considerable. For example, the room temperature lattice thermal conductivity of a compound of composition $C_{24}M$ should be about 0.03 of that of graphite in the C-direction.

Thermoelectric Effects in Graphite Alloys

Senior Investigator: Dr. S. Pollack

Graduate Student: J. Curry

During the past three months, the apparatus for the measurement of the thermoelectric power has been completed. The variable temperature system consists of a bottom dewar to hold liquid nitrogen, a copper rod and heater assembly, the sample holder, and an inverted dewar to cover the rod and sample holder. A temperature differential is established across the sample by means of a small heater at one end of the sample holder. The other end is mounted to the rod-heater assembly. With this system it is possible to measure the thermoelectric power (as well as other transport properties by the interchange of sample holder) from $77^{\circ}K$ to $400^{\circ}K$. Temperature differential is measured by two thermocouples connected to isolated DC amplifiers which drive on pen of a 2 pen X-Y recorder. The Seebeck voltage, ΔE, is measured by a microvoltmeter which drives the other pen of the recorder. The X axis is driven by the thermocouple in the cold junction.

The plots obtained are those corresponding to ΔE vs. T and ΔT vs. T. A computor program has been written to perform the necessary computations. The sensitivity of the apparatus is such that temperature differences have been resolved to the nearest $0.1K^{\circ}$ at $77^{\circ}K$ and $0.03K^{\circ}$ at room temperature. This arises from the change in thermoelectric power of the thermocouple with temperature. The Seebeck voltage can be measured with a sensitivity of 0.01 microvolts from 0-100 microvolts and a sensitivity of 0.01 millivolts from 0.1 to 100 millivolts. Currently the apparatus is being used to

measure the thermoelectric power of substances whose thermoelectric power is well known and accepted for the purposes of calibration.

During the next three months, the sample holder for the measurement of conductivity, Hall coefficient and magnetoresistivity will be completed. The system has been designed to be used with the high field magnet available in the Laboratory for the Research on the Structure of Matter. Using this system it will be possible to generate continuous data on the transport properties of graphite alloys rapidly and accurately.

Tunnel Emission Cold Cathodes

Senior Investigator: Dr. S. Pollack

Graduate Student: S. Basavaiah

Since the previous report this Project has faced a number of major problems. After the VEECO electron beam gun had been installed into the Elion vacuum system, attempts were made to evaporate tungsten by electron bombardment. The pressure in the system increased excessively high. Without evaporation the pressure was about 5×10^{-7} torr. As soon as the electron beam was turned on, the pressure increased and went up to about 10^{-4} torr for a beam power of 2.75 k.w. It required, as we found out, more than 3 k.w. to evaporate tungsten. Since the gun cannot be operated at 10^{-4} torr, further increase in power was not possible.

Meanwhile the vacuum system developed a leak in one of the weldments.

Some modifications were made in the shape and mounting of the tungsten piece to provide better heat shielding and isolation, but without any success. To complicate the problem, the titanium rubbimation pump was found to be completely ineffective. It was concluded that due to the inherent size of the bell jar (30"x30") and large amounts of gas load due to high temperature required for tungsten evaporation the existing vacuum chamber could not be used. It was decided to replace the bell jar.

Mr. Basavaiah took a leave of absence from 8 June to 26 August 1966. Prior to his leaving, a Varian stainless steel bell jar 18"x36" with standard conflat flanges and a Wheeler flange was designed. A far more efficient titanium sublimation pump with cryo-panel was included.

A more effective roughing line using the existing 1397 Welsh pump was also included. The control panel, ion pump, gate valve, and

mechanical pump of the Elion system has thus been retained. This system has been under construction since July and was shipped from California on September 21st. In the interim the internal jigging, and water cooled sample holder were redesigned to fit into the smaller vacuum chamber.

The completed system should be operative by October 15th.

Studies of Thermal Transpiration for the Development of a "Thermal Pump"

Dr. M. Altman, Mr. E. Hopfinger

A temperature gradient across a porous membrane, placed in a gas, with a pore size smaller than the mean free path of the gas causes a pressure gradient to develop, according to the relation $P_1/P_2=(T_1/T_2)^{1/2}$, where P_1, P_2 and T_1, T_2 are the pressures and temperatures at the two surfaces of the membrane. This phenomenon is called "thermal transpiration". If the two chambers, which are separated by the membrane, are joined by a tube of a diameter much larger than the mean free path, a continuous flow is established. This is in principle a "thermal pump".

In earlier studies of non-isothermal molecular flow through porous media at low mean pressures (about 1 cm Hg) the above pressure-temperature relation was verified (1), (2). The same relation is true if the porous medium is replaced by capillaries (3), (4).

Since the efficiency of a thermal pump will vary proportionally to the pressure at which it operates, it is desirable to carry out investigations at atmospheric pressures. The aims of the present investigations are therefore:

a. To verify the validity of the above pressure-temperature relation at atmospheric pressures and relatively high temperatures in membranes at appropriately fine pores.

b. To determine the optimum conditions for flow rates.

The flow rates through an infinitely thin membrane can be calculated from kinetic theory. These rates are very high. A plot of flow rates versus temperature difference is shown in the following graph.

Figure 1

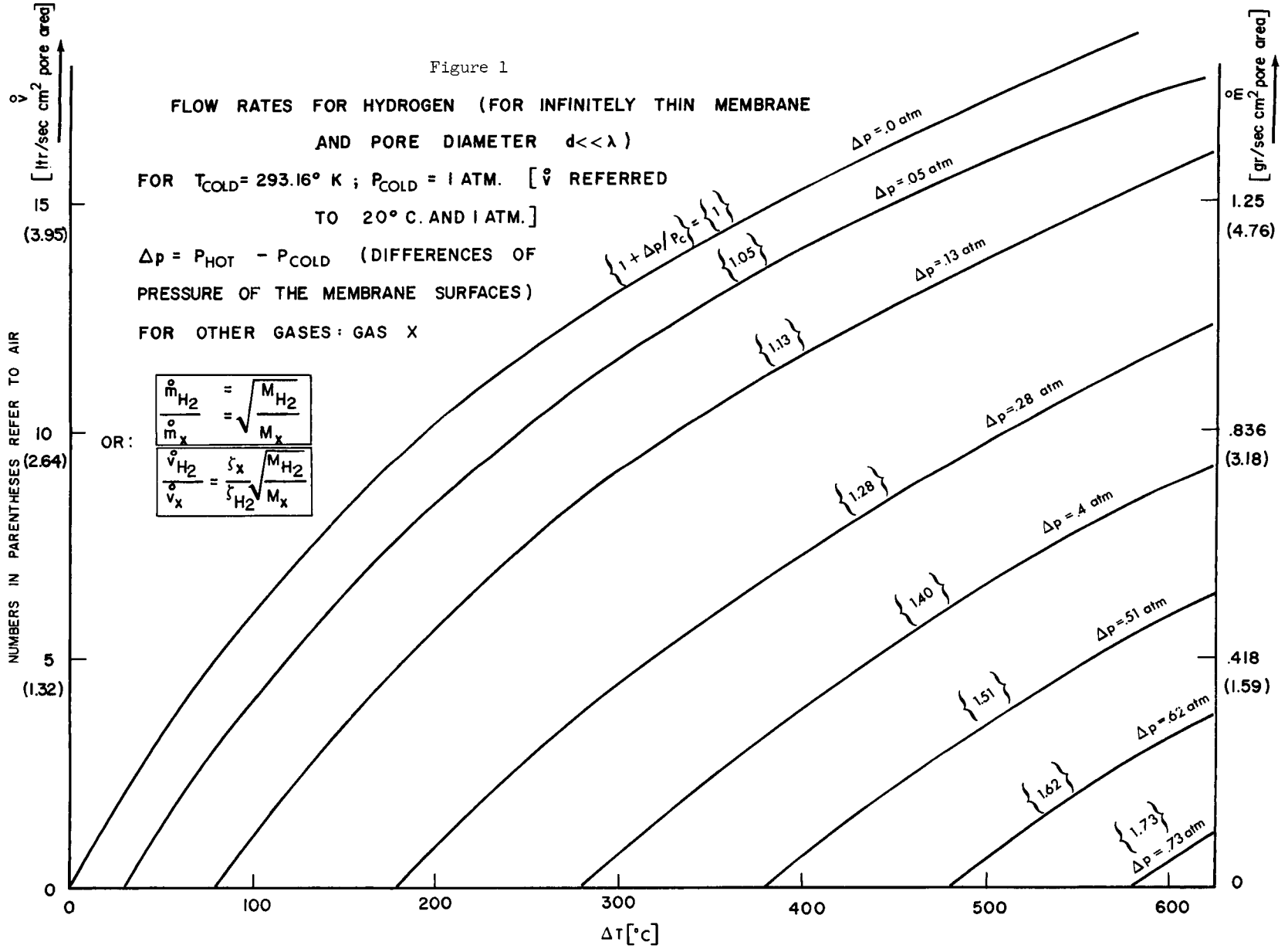
FLOW RATES FOR HYDROGEN (FOR INFINITELY THIN MEMBRANE AND PORE DIAMETER d<<λ)
FOR T_COLD = 293.16° K ; P_COLD = 1 ATM. [v̊ REFERRED TO 20° C. AND 1 ATM.]
Δp = P_HOT − P_COLD (DIFFERENCES OF PRESSURE OF THE MEMBRANE SURFACES)
FOR OTHER GASES: GAS X
OR:
ṁ_H2 / ṁ_x = √(M_H2 / M_x)
v̊_H2 / v̊_x = (ζ_x / ζ_H2) √(M_H2 / M_x)
v̊ [ltr/sec cm² pore area]
ṁ [gr/sec cm² pore area]
NUMBERS IN PARENTHESES REFER TO AIR
Δp = .0 atm
Δp = .05 atm
Δp = .13 atm
Δp = .28 atm
Δp = .4 atm
Δp = .51 atm
Δp = .62 atm
Δp = .73 atm
{1 + Δp/P_c} = {1}
{1.05}
{1.13}
{1.28}
{1.40}
{1.51}
{1.62}
{1.73}
15 (3.95)
10 (2.64)
5 (1.32)
0
1.25 (4.76)
.836 (3.18)
.418 (1.59)
0
0
100
200
300
400
500
600
ΔT[°C]

Flow Rates for Pressures P_{cold} different from 1 atm

$$\dot{m}_{H_2} = 62.8 \left[P_c/\sqrt{T_c} - P_H/\sqrt{T_H} \right]$$

$$= 62.8\, P_c \left[\frac{1}{\sqrt{T_c}} - \frac{P_H/P_c}{\sqrt{T_H}} \right]$$

$$\dot{m}_{H_2} = \frac{62,8}{\sqrt{T_c}} P_c \left[1 - \sqrt{\frac{T_c}{T_H}} \left(1 + \frac{\Delta p}{P_c} \right) \right]$$

here $\left(1 + \frac{\Delta p}{P_c} \right) = P_H$

Procedure:

a) Calculate quantity $(1 + \Delta p/p_c)$

b) Pick corresponding curve in ΔT - $\dot{m}$ plot and read off $\dot{m}$ at the ΔT.

c) Multiply $\dot{m}$ by P_c (in [atm])

In an experimental setup the membrane will have finite thickness and therefore the flow rates will be dominated by thermal diffusion within the membrane. This will cause the flow rates to decrease considerably. (5) (6).

Initial experiments, which consisted of pressing a very fine powder into a 1 inch diameter porcelain tube, one side of which was then closed off and the other one heated to high temperature, were quite encouraging. One porous plug made in this way of diatomacheous earth was about 2 inches long. The closed end of the tube was connected to a manometer and the open end was heated to about 700°C. The pressure dropped in one minute by 1.6 cm and in 3 minutes by 3.7 cm, and reached a maximum of 7.2 cm after about 20 minutes. The above was repeated with MgO powder of .06 microns particle size and a maximum pressure drop of 11.5 cm was recorded.

At present an apparatus is being developed which will permit investigation of the transpiration phenomena and membranes of various pore sizes and thicknesses at various mean pressures and temperature differences (up to 500°C).

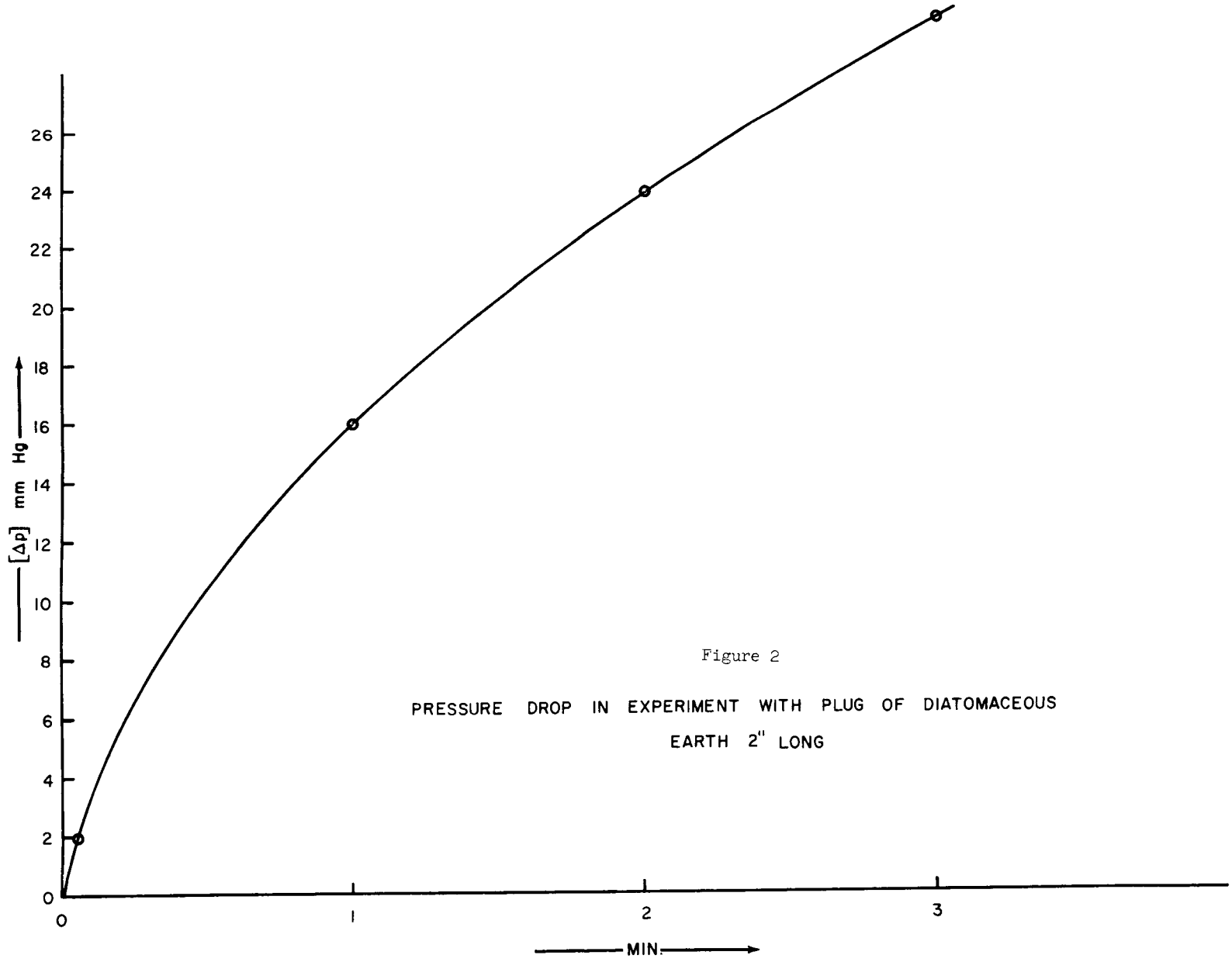

Figure 2

PRESSURE DROP IN EXPERIMENT WITH PLUG OF DIATOMACEOUS EARTH 2" LONG

References

1. O. Reynolds, Phil. Trans. Roy. Soc. (London) B170, 727 (1879).
2. J. M. Hanley, J. Chem. Physics, 43, 1510, (1965).
3. Liang, Can. J. Phys. 33, 279 (1955).
4. Edmunds and Hobson, J. Vac. Sci. Technol., 2, 182 (1965).
5. H. Ebert and K. R. Albrand, Vacuum, 13, 563 (1963).
6. E. Mason, R. Evans, G. Watson, J. Chem. Phys., 38, 1808 (1963).

PLASMA ENGINEERING

APPENDIX 3

Plasma Diagnostics - Slow Wave Plasma Diagnostics

L. W. Zelby, W. Becker

Work on refinement of slow-wave plasma diagnostics has continued. Previous work (INDEC-SR-8*) indicated that dispersion relations, and phase shift measurements alone, are ambiguous. To remove this ambiguity, attenuation measurements are also needed. To determine changes in attenuation due to spatial variations of electron-neutral collision frequencies, the helix-plasma column problem was solved assuming collision frequency variations of the form

$$\nu = \nu_0 \left[1 - \delta_2 (r/a)^m\right]$$

Attenuation, with δ_2 and m as parameter, vs frequency is plotted in Fig. . Increasing m and decreasing δ_2 increases the attenuation and leads to an ambiguity, as seen in the figure. This points up the need for the combined measurements to determine the plasma parameters uniquely.

Measurements of attenuation and phase shift on plasma columns of different diameters are planned for the next period.

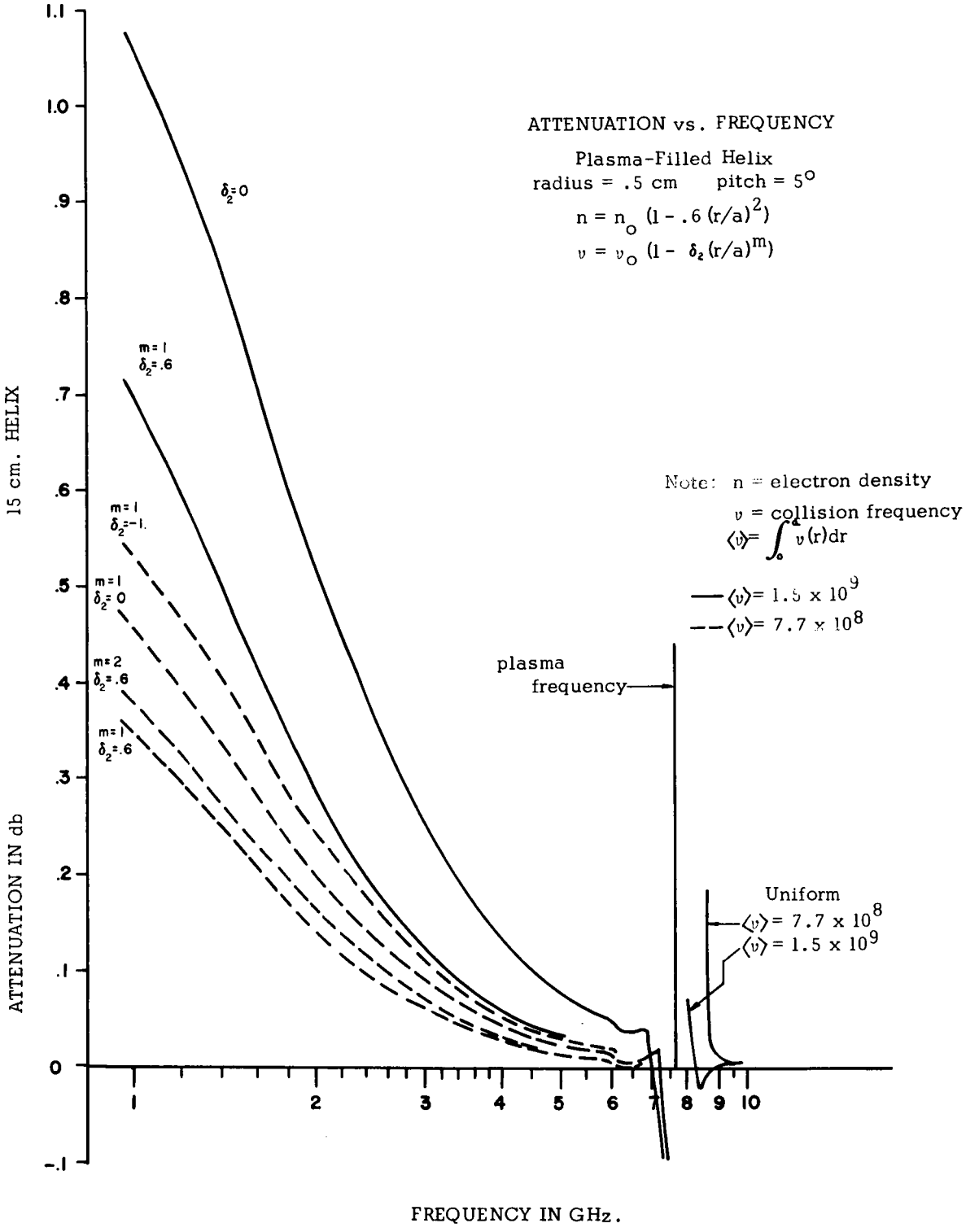
ATTENUATION vs. FREQUENCY
Plasma-Filled Helix
radius = .5 cm pitch = 5°
$n = n_o (1 - .6 (r/a)^2)$
$\nu = \nu_o (1 - \delta_2 (r/a)^m)$
Note: n = electron density
ν = collision frequency
$\langle\nu\rangle = \int_0^a \nu(r)dr$
$\langle\nu\rangle = 1.5 \times 10^9$
$\langle\nu\rangle = 7.7 \times 10^8$
plasma frequency
Uniform
$\langle\nu\rangle = 7.7 \times 10^8$
$\langle\nu\rangle = 1.5 \times 10^9$
$\delta_2 = 0$
m = 1 $\delta_2 = .6$
m = 1 $\delta_2 = -1.$
m = 1 $\delta_2 = 0$
m = 2 $\delta_2 = .6$
m = 1 $\delta_2 = .6$
15 cm. HELIX
ATTENUATION IN db
FREQUENCY IN GHz.
1.1
1.0
.9
.8
.7
.6
.5
.4
.3
.2
.1
0
-.1
1
2
3
4
5
6
7
8
9
10

Transport Properties of Partially Ionized Gases - The Tensor Electrical Conductivity of Atmospheric Cesium-Seeded Argon

S. Schweitzer

The third Chapman-Enskog approximation to the tensor electrical conductivity of a partially ionized gas was used to evaluate two mixture rules. The so-called mean-free-path mixture rule and a recently proposed integral-mixture rule were examined for cesium-seeded argon at atmospheric pressure in the temperature range of $1400^{\circ}K$ - $3000^{\circ}K$. Upper and lower bounds of actual electron-neutral cross sections were used in the calculations. It is shown that under certain conditions of seeding and Hall parameter values the integral-mixture rule may yield results that should be correct within 20%. The effect of uncertainties in electron-neutral cross sections was shown to diminish with increased values of the Hall parameter.

Details of the research were submitted for journal publication.

Surface Physics - The Influence of High Fields on Surface Charge Distributions

G. L. Schrenk, S. Fonash

Research on the influence of high electric fields on surface charge distributions has been initiated with respect to two specific phenomena.

The first concerns regions of varying average intensity frequently observed in field ion micrographs. These regions are sharply defined and are more pronounced in some metals than in others. In platinum, they form one of the most prominent features of the micrograph. Preliminary theoretical research is under way to see whether this effect can be explained.

The second concerns electron charge distribution of surface atoms ("kinks") with respect to field ion microscopy. It is often stated that only "kink" atoms are imaged in the microscope; but rigorous definition of what constitutes a "kink" atom has not been developed. Several empirical relations between the geometry of spherical crystals and the number of broken bonds have been proposed with some success. Preliminary theoretical research is under way to determine the relation between these empirical formulas and physical principles. Specifically, three-dimensional quantum mechanical tunneling in the presence of high electric fields is considered. This includes the effects of both: the electron charge distribution of surface atoms, and the local electric fields.

Surface Physics - Anisotropy of Metal Work Functions
in Extremely High Electric Fields

M. Kaplit

Work to resolve the difference in two measurements of the work function of the (110) face of tungsten continues. The difference is at least 0.6 ev between the two measurements: thermionic emission and field emission probes. Preliminary results (INDEC-SR-8) were presented at the 13th Field Emission Symposium.

Figures 1 and 2 show the calculated mechanical surface stress and surface atom polarizability of tungsten as functions of the applied electric field and crystallographic orientation. For field desorption conditions (electric fields $\approx$ 1 V/Å to 10 V/Å), it was found that the surface stresses are of the same order as the tensile strength and that the polarizabilities are somewhat less than the volume of a tungsten atom (≈ 3.5 Å^3). The results for the (110) and (211) face are very small because of an exaggerated effect of charge spreading.

Present work is directed towards understanding the effect of surface charge spreading on work function changes.

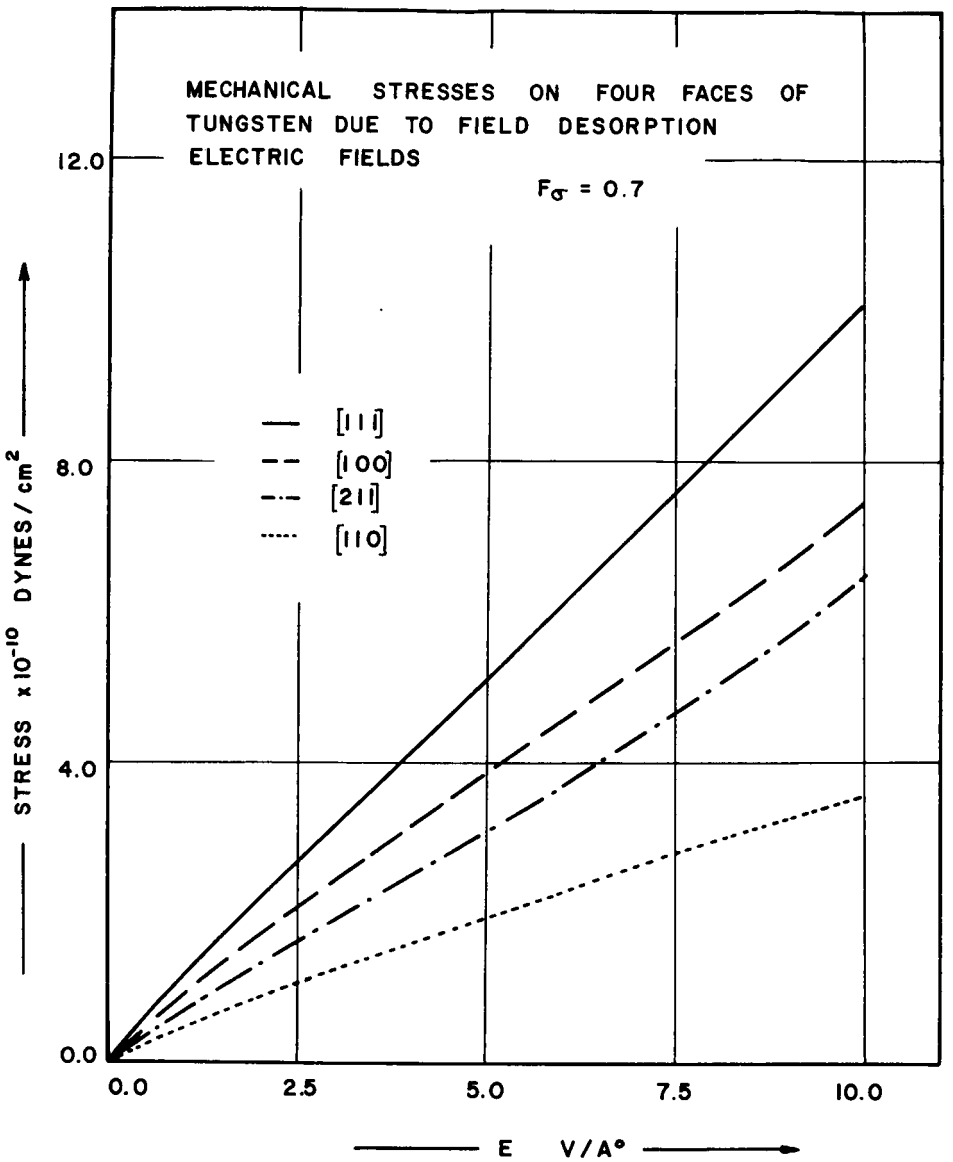
MECHANICAL STRESSES ON FOUR FACES OF TUNGSTEN DUE TO FIELD DESORPTION ELECTRIC FIELDS
F_σ = 0.7
[111]
[100]
[211]
[110]
STRESS x 10^{-10} DYNES / cm^2
12.0
8.0
4.0
0.0
0.0
2.5
5.0
7.5
10.0
E V/A°

Figure 1

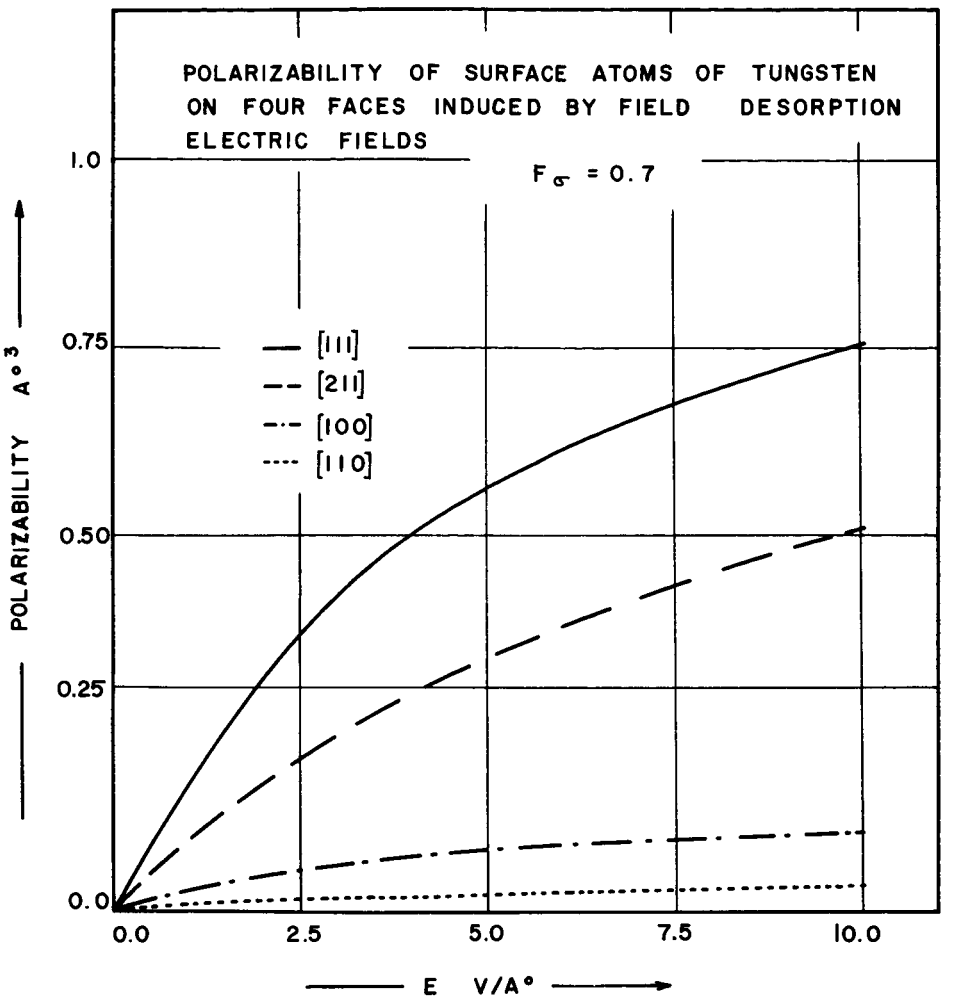
POLARIZABILITY OF SURFACE ATOMS OF TUNGSTEN
ON FOUR FACES INDUCED BY FIELD DESORPTION
ELECTRIC FIELDS
F_σ = 0.7
[111]
[211]
[100]
[110]
POLARIZABILITY A°³
1.0
0.75
0.50
0.25
0.0
0.0
2.5
5.0
7.5
10.0
E V/A°

Figure 2

Thermionic Converters - Characteristics of Thermionic Plasma Diodes with Gas Mixtures

G. L. Schrenk, A. Kaufman

The purpose of this work is the investigation of effects of gas mixtures which exhibit the Penning effect on the performance of plasma diodes.

Work on calculations of the electron-atom excitation and ionization cross sections, and the Penning cross sections, for cesium-cadmium and cesium-mercury systems is continuing. Mathematical models for both the ignited and the unignited mode of a plasma diode using a gas mixture are near completion. Currently, our attention is focused on the transition region between these two modes for the purpose of understanding the difference between the operating points of plasma diodes with gas mixtures and the more conventional plasma diodes.

Plasma Centrifuge

M. Altman S. Schweitzer

P. Hsueh

The purpose of this project is the study of the motion of an incompressible, constant-viscosity, electrically conducting fluid, confined between two concentric cylinders and driven by electromagnetic forces (configuration and the applied fields were presented in the previous reports). The analysis will include consideration of the effects of variation of parameters of the system and of heat transfer; rotational and secondary flow phenomena; and the feasibility of practical application.

The theoretical analysis of the problem has been completed. In the case of small magnetic Reynolds number, and negligible Hall effect, following results were obtained:

1. Flow field in an infinitely long cylinder expressed in terms of Bessel functions was compared with the corresponding inviscid solution. For Hartmann numbers much larger than the first eigenvalue, the solution approaches that of the inviscid case, in which the rotational velocity is inversely proportional to the applied magnetic field. For Hartmann numbers much smaller than the first eigenvalue, the rotational velocity becomes proportional to the applied magnetic field. It was also found that the energy storage, and the ultimate flow velocity, reach their maximum when the Hartmann number is comparable to the first eigenvalue. Figure 1 shows this result.

2. The flow approaches steady state exponentially as

where

ν is the kinematic viscosity

λ_n are the eigenvalues

M is the Hartmann number

d is the gap between the two cylinders

t is the time.

Numerical results show that for mercury, with $r_1=6x10^{-2}m$, $r_2=12x10^{-2}m$, in magnetic induction of 500 gauss and voltage difference of $5x10^{-3}$ volts, the rotational velocity can reach the steady state, 1m/sec or 120 rpm, in 22 seconds.

3. The heat generated by Joule heating and viscous dissipation were considered to be the only heat sources in the field. Radiation boundary conditions were used to obtain a general solution. The temperature distribution and the amount of heat being generated depend mainly on the material properties of the fluid. For the case considered above, since the mercury has low resistivity and low viscosity, very little heat is generated. The temperature distribution for both boundaries kept at room temperature is shown in Figure 2, indicating that for most liquid materials, little heat will be generated.

4. Perturbation technique was used to study the effects due to the induced fields. It was found that a secondary flow will be generated in the direction perpendicular to that of the rotational flow. The numerical results of the analytical solution expressing the secondary flow were calculated with rotational and the secondary flow pattern shown in Figure 3.

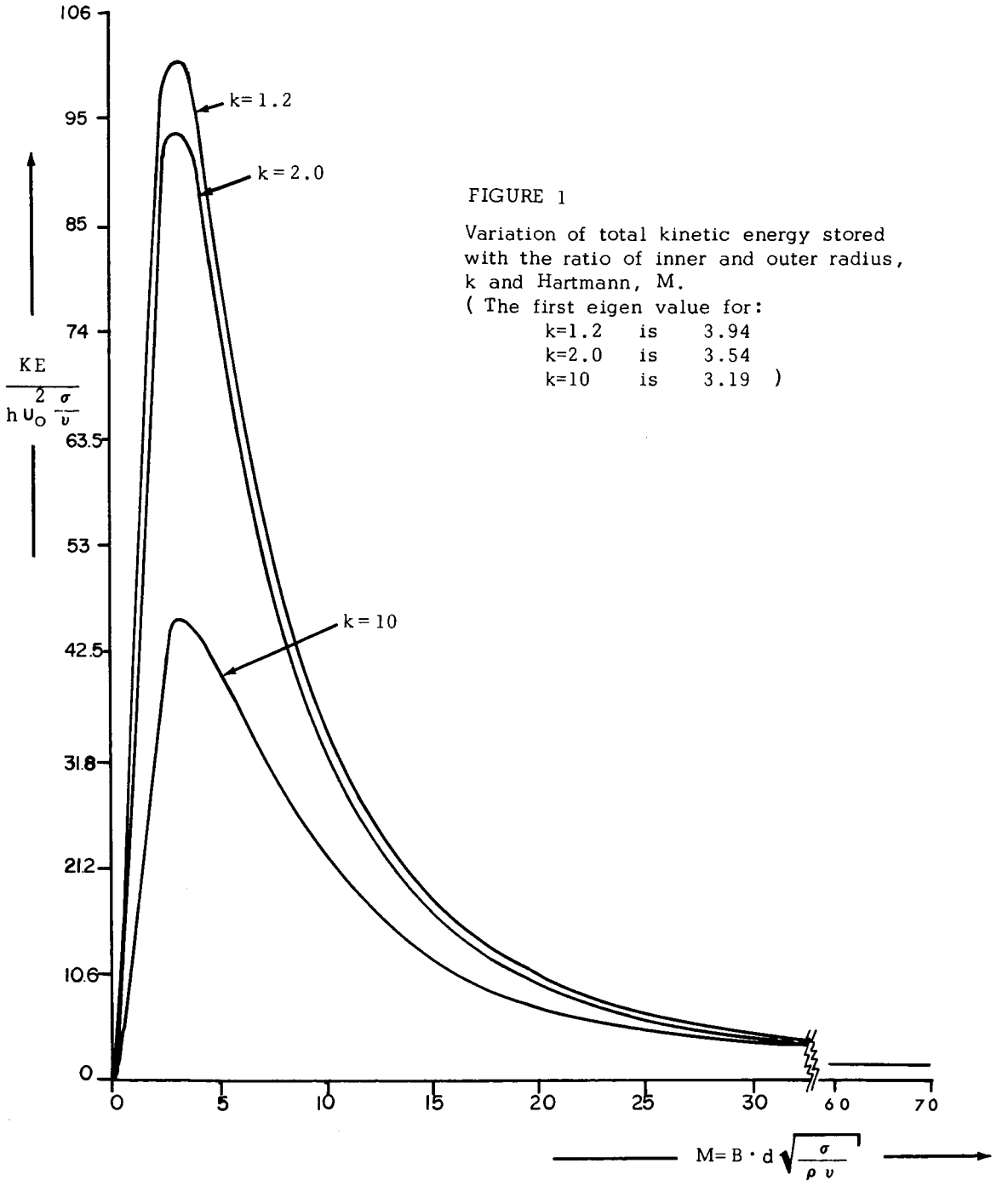

FIGURE 1

Variation of total kinetic energy stored with the ratio of inner and outer radius, k and Hartmann, M.
(The first eigen value for:

k=1.2	is	3.94
k=2.0	is	3.54
k=10	is	3.19)

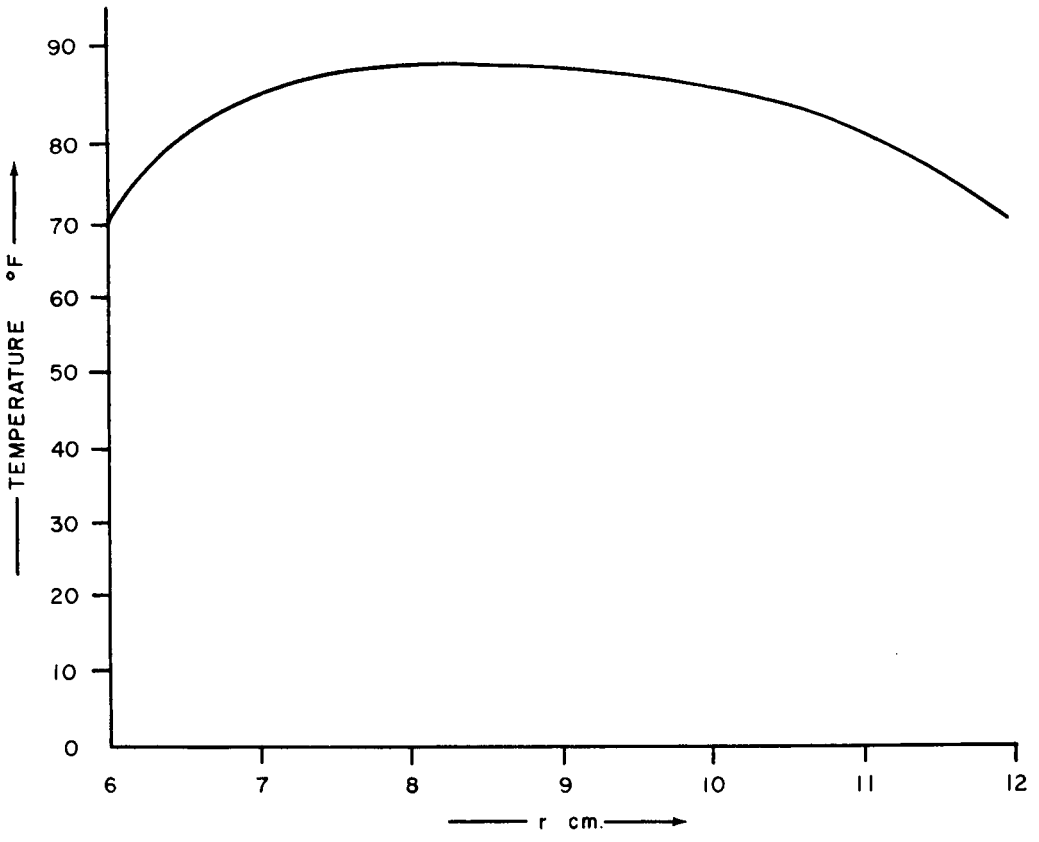

FIGURE 2. TEMPERATURE DISTRIBUTION OF MERCURY FOR

Inner radius = 6×10^{-2} m

Outer radius = 12×10^{-2}

Applied magnetic = 500 gauss

Applied electric potential = 5×10^{-3} volts.

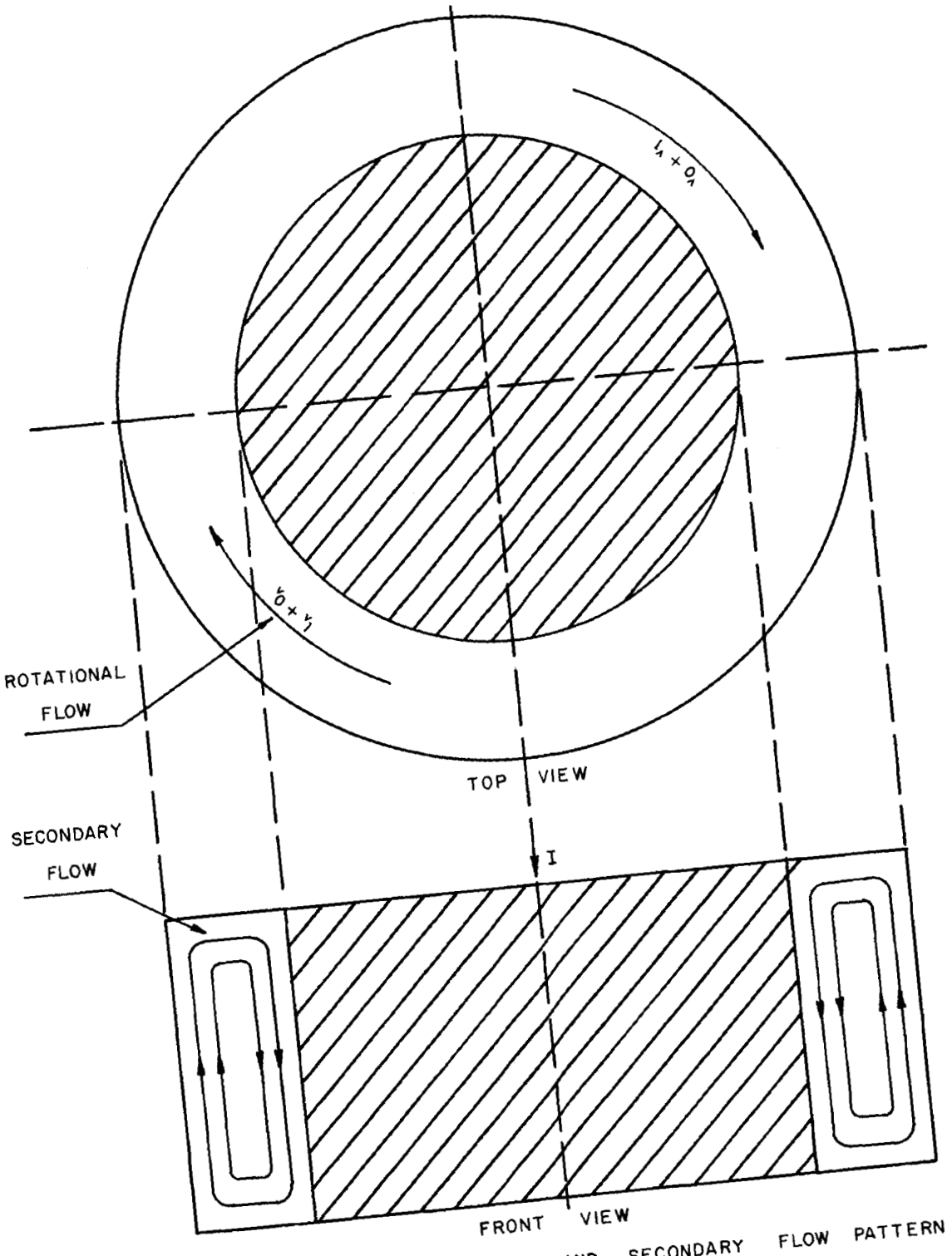

FIGURE 3 – A TYPICAL ROTATIONAL AND SECONDARY FLOW PATTERN

ELECTROCHEMICAL ENGINEERING

APPENDIX 4

Atomic Scale Electrode Processes

Dr. P. Javet, Dr. L. Nanis

The field ion microscope (FIM) opens to the electrochemist a new approach to the study of electrocatalysis. It permits one to see the electrode on an atomic scale and to observe the transformations occurring as a result of electrochemical treatments. Owing to the lack of previous published work and information concerning this particular application of FIM, we have chosen to begin with the most simple device on the market - the "Müller FIM", produced by the Central Scientific Corporation. Designed as a teaching device for advanced physics students, this microscope has required some improvement and modification. The following results have been obtained:

a. Tungsten

Although tungsten may not be of great electrochemical interest in itself, a preliminary study of this metal has been undertaken because two particular aspects are of interest. They are:

(1) As a refractory metal with very high melting point, W is the most appropriate metal to obtain good FIM images. Particularly, the best image voltage (BIV), at which the image is at maximum resolution, and the field evaporation voltage (FEV), at which some atoms are removed from the surface, are rather different (FEV = BIV + 20%). As such, the W can be considered as a very favorable metal for FIM in general.

(2) Owing to the behavior of W mentioned above, W tips can be used as holder for other metals to be investigated by FIM (which can be deposited on W tips by various techniques - particularly by electrochemical deposition, e.g.,of platinum). The results obtained with W have confirmed the behavior mentioned above. We have obtained very

clear pictures of W tips, showing in the best cases full resolution of the chain of atoms in the (110) region (line resolution ~ 2.2 Å), and resolution of the atom itself in some higher index planes such as (122) (point resolution: 4.5 Å), or even (112) (point resolution: 2.8 Å).

The obtained resolution, which is really good for this device, shows that the experiments we intend to conduct are actually feasible with this FIM and W tips.

b. Platinum

The interest we give to the investigation by FIM of Pt is principally due to the following points:

(1) Many electrochemical devices in research fields as well as in practice (fuel cells) use Pt electrodes. The Electrochemistry of this metal is also well studied.

(2) The high catalytic power of Pt, together with its ability to adsorb foreign molecules, can be studied very properly by FIM and is directly related to the electrochemical behavior of Pt.

(3) Platinum has been proven to be one of the metals which can be studied by FIM, and many references on such studies can be found in recent literature. However, Pt is for FIM a less favorable case than W owing to the fact that the BIV is very close to the FEV. The ordinary assumed value for the difference is only a few percent.

The results obtained so far with Pt have shown that the study of this metal with FIM is much more difficult than for W. As yet, we have not reached with Pt the satisfactory resolution we have reported above for W. In the best cases, we have obtained resolutions over limited regions of rows of atoms (but not of the atoms themselves) for different crystallographic directions. The reason for this limited resolution seems to be a complex combination of the following factors:

(1) Small difference between BIV and FEV.

(2) Gaseous contamination which seems to be hard to remove with the present pumping system.

(3) Bad shape of the tips which seem to be either well annealed but showing too great a radius of curvature, or with proper radius, but unannealed, with atoms very irregularly distributed.

The second of the above mentioned points is being corrected with a new device for filling of the microscope tube with imaging gas (helium). If needed, a purification stage of the gas will be added. Furthermore, this new device will allow the use of other imaging gases (Ne) or of mixture of gases, which increases the difference between BIV and FEV for platinum. The goal remains as before - namely, the determination of oxygen adsorption coverage on Pt as a function of applied electrochemical potential. Pure iridium tips will also be studied since its electrochemical behavior can be expected to be similar to platinum.

Freezing Potentials

Dr. L. Nanis, Mr. I. Klein

The effect of substrate on the freezing potential phenomenon was investigated in the following manner - a 0.4 ml droplet of various solutions (2.5×10^{-4} N, 2.5×10^{-5} N, 2.5×10^{-6} N NH_4Cl, and 5×10^{-4} N NaCl) was alternately placed on five different substrate surfaces (silver, silver covered with a thin layer of silver chloride, copper, aluminum oxide, and platinum) and subsequently frozen. Data such as the freezing potential, the freezing time, and the potential of the system prior to freezing were obtained, and they are indicated in Table 1. The experimental apparatus was so designed that the reference electrode was fed into the input of the electrometer while the metal substrate was connected to its ground, so one must accordingly take care when interpreting the signs of the tabulated voltages, i.e., if a negative voltage is recorded, then the substrate is positive with respect to the reference electrode and vice versa. Note also that the recorded freezing potentials are the maximum voltages observed during a particular freezing run.

An examination of Table 1 immediately corroborates the original assumption that the substrate does indeed affect the resulting freezing potential. By altering the substrate, for a given solution, one changes the rate of freezing as well as the initial cell potential and it is hypothesized that these two factors in turn influence the freezing potential.

The effect of the initial cell potential (before freezing) is secondary to the more dominant effect of variable freezing time. A graph of the mean freezing time versus the mean freezing potential is shown in Fig. 1. It may be seen that for any given concentration there exists an optimum freezing time which maximizes the freezing potential. This optimum time

appears to vary as an inverse function of concentration. Furthermore, at optimum freezing times, the magnitude of the resulting freezing potential varies inversely with the concentration.

These aforementioned observations, if correctly interpreted, constitute a basis upon which one might build a theoretical mechanism that ultimately explains the nature of freezing potentials. The preliminary studies that have been performed indicate that these voltages are the result of a complex interaction of several phenomena, including zone refining characteristics of charged ions - e.g.,diffusion of ions in the double layer under the influence of an electrical field and the orienting effect of the substrate. An attempt will be made to evaluate the freezing potential mechanism by determining which of these phenomena are of primary importance and their functional relationship. At present, data is being sought in the literature for potentials of zero charge in order to evaluate the metals so far studied. Also under study is a separate determination of thermal time lags for the sheet metal substrates.

TABLE 1

MAXIMUM FREEZING POTENTIAL DATA

AMMONIUM CHLORIDE*

Substrate	2.5×10^{-4}N F.P.	2.5×10^{-4}N F.T.	2.5×10^{-4}N I.P.	2.5×10^{-5}N F.P.	2.5×10^{-5}N F.T.	2.5×10^{-5}N I.P.	2.5×10^{-6}N F.P.	2.5×10^{-6}N F.T.	2.5×10^{-6}N I.P.
Ag	-.38 ∓ .13	60 ∓ 2	.065 ∓ .011	-5 ∓ 2	58 ∓ 6	.059 ∓ .014	-3 ∓ 3	56 ∓ 11	.065 ∓ .018
Ag-AgCl	-1.1 ∓ .5	59 ∓ 6	.008 ∓ .002	-8.3 ∓ 2.0	62 ∓ 6	.009 ∓ .004	-11 ∓ 4	52 ∓ 6	.010 ∓ .002
Cu	-.16 ∓ .01	64 ∓ 5	.26 ∓ .06	-13 ∓ 5	76 ∓ 9	.21 ∓ .01	-7 ∓ 4	65 ∓ 9	.22 ∓ .02
Al_2O_3	.22 ∓ .15	88 ∓ 16	.73 ∓ .06	-14 ∓ 6	99 ∓ 10	.65 ∓ .03	-40 ∓ 20	114 ∓ 13	.75 ∓ .11
Pt	-.8 ∓ .4	111 ∓ 9	.05 ∓ .02	-4.9 ∓ 1.4	125 ∓ 21	.09 ∓ .02	-13 ∓ 6	150 ∓ 20	.06 ∓ .03

SODIUM CHLORIDE

Substrate	5×10^{-4}N F.P.	5×10^{-4}N F.T.	5×10^{-4}N I.P.
Ag	2.6 ∓ 1.2	57 ∓ 9	.09 ∓ .03
Ag-AgCl	8.2 ∓ 1.5	57 ∓ 3	.006 ∓ .002
Cu	3.6 ∓ 1.7	70 ∓ 11	.17 ∓ .02
Al_2O_3	3.8 ∓ 1.3	104 ∓ 16	.62 ∓ .11
Pt	8.9 ∓ 1.4	138 ∓ 16	.04 ∓ .04

*All parameters are given with plus and minus standard error based on the standard deviation of all data obtained in replicate studies.

F.P. Freezing Potential, Volts
F.T. Freezing Time, Seconds
I.P. Initial Potential, Volts (vs. Ag/AgCl)

Effect of Freezing Time on Freezing Potential

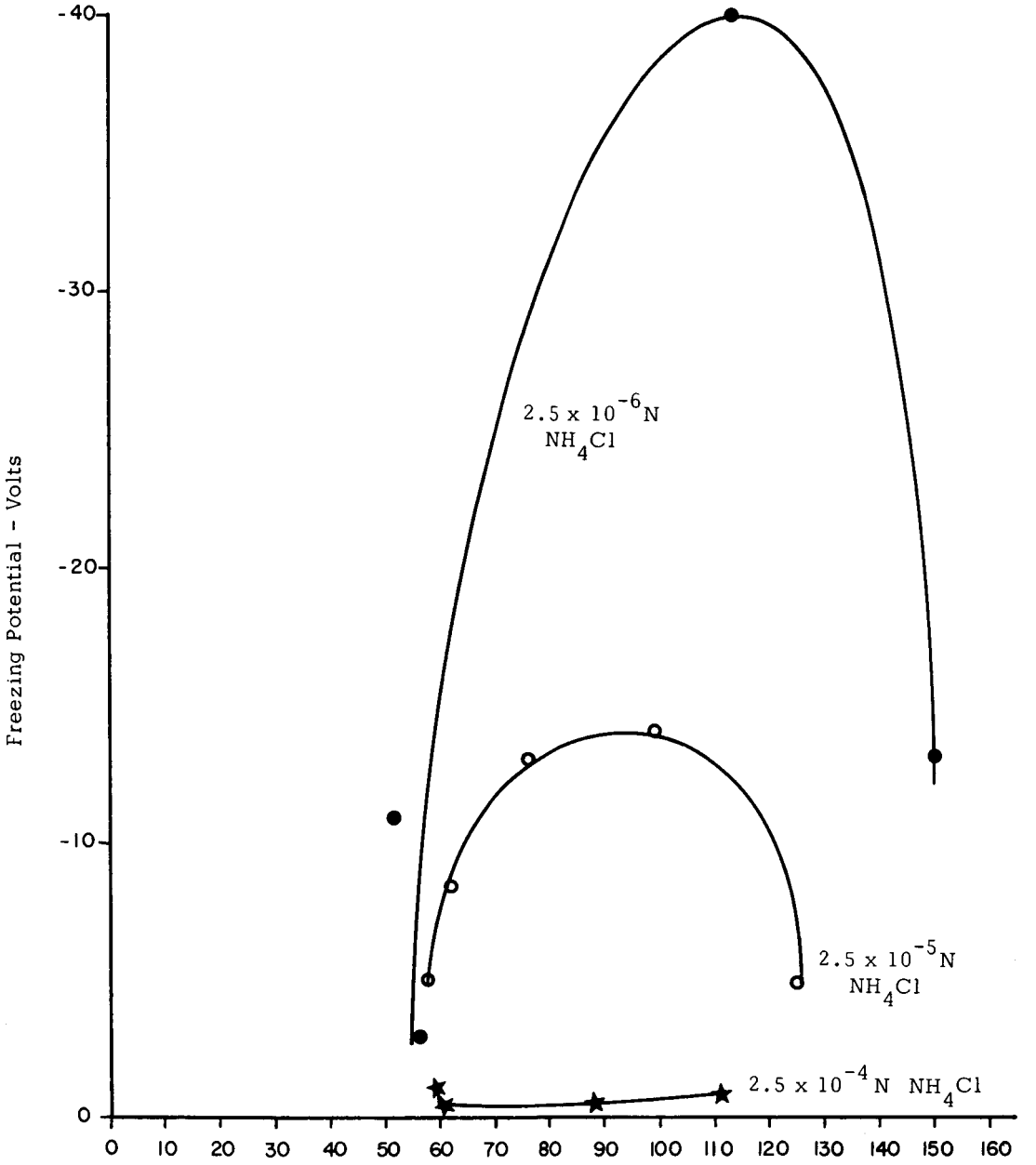

Figure 1

Studies of Platinum Fuel Cell Electrodes

Dr. L. Nanis, Mr. G. Rowell

The study of the voltage decay of a platinum anode in 1N H_2SO_4 was continued using the same apparatus as described in the last Status Report (INDEC-SR-8). Experiments were run to determine the effect of hydrogen gas on the voltage decay plateau and on the voltage decay and to study the wetting characteristics of the electrolyte at different voltages and surface conditions.

Decay experiments were made after the anode was charged for six minutes at a current density of 0.17 mA/cm^2. Throughout the experiments, blank runs were made in which the voltage following current interruption was allowed to decay normally for comparison with treated runs. A treated run consisted of the normal charging period followed by current interruption, and, when the voltage had decayed to the plateau voltage, the electrolyte level was dropped, exposing the new surface to flowing hydrogen. After a specified time, the liquid was raised and the voltage decay allowed to continue. Typical results of these experiments can be seen in Fig. 1 which is a plot comparing a few treated runs to blank runs. It may be clearly seen that there are definite differences between normal decay and decay following exposure to hydrogen gas. Firstly, there is a voltage hold in the blank runs at 0.740 volts, whereas, after hydrogen treatment, the voltage never reaches this plateau and almost immediately starts to decay. In the treated decay curves, the voltage drops much sooner at an initially faster rate and reaches its maximum decay rate at 0.51 volts. For the blank runs, there was a hold at the voltage plateau, after which the voltage began to decrease slowly followed by a rapidly increasing rate reaching a maximum at 0.42 volts.

It should be noted that the maximum decay rate for the blank was much greater even though it was reached at a later time and lower voltage. Both curves approached an exponential decay at the lower voltage range with the slope of the blank being the greater of the two. Tentative conclusions from these results are that the hydrogen treatment removes the oxide layer causing the voltage to come off of the voltage plateau and that the mechanism for the decay is changed by this hydrogen treatment.

The second experiment was a study of the effects of hydrogen on some of the surface characteristics of the electrode. It was noted during operations of the above experiment that when lowering the liquid with the electrode maintained at 1.5 volts (NHE) a film clung to the surface as in a good wetting situation, while when lowering the liquid level with the electrode at lower voltages, a beading effect was noted as in poor wetting. Therefore, after charging (similar to the decay experiments), the liquid was lowered at different voltages to find the transition between the two types of wetting. Also the liquid level was raised into the area of the electrode that was in contact only with hydrogen gas and had never been charged. The results showed that the transition from good to poor wetting occurred between 0.72 volts to 0.76 volts. In the second part of the experiment, the voltage rose to 0.66 volts when the liquid level was raised into the previously unwetted section. When lowered, the wetting was similar to the low voltage type and the potential of the lower section of the electrode normally used was only 0.03 volts (NHE). The tentative conclusions that are reached from these results are that the change of wetting characteristics coincides with the plateau voltage, possibly corresponding to a disappearance of the platinum oxide layer. The existence of a platinum oxide layer is associated with good wetting. Thus the open circuit potential of 0.66

volts attained by covering fresh electrode surface with electrolyte might be ascribed to a mixed potential over the entire electrode caused in part by the oxide region. But, since the film draining from the new region (upper section of electrode) indicates the absence of oxide, the potential increase must be associated in some way with hydrogen coverage. Thus, the decay curves shown in Fig. 1 are chiefly a function of hydrogen behavior and not platinum oxide. Mechanisms to explain the slow decay of electrode potential following exposure to hydrogen gas are being considered presently in the light of previous models of this system [H. Dietz, H. Göhr, Electrochimica Acta, V. 8 (1963) p. 343] where the sequence of electrode polarization is considered to involve the sequential steps of hydrogen desorption, oxygen adsorption, platinum oxide formation and oxygen evolution. It should be noted in Fig. 1, for interrupted curve 2, that hydrogen exposure at the very start of potential plateau behavior apparently decreases the length of plateau time but has little effect on the potential, which may be seen to recover nearly to the previous value. However, the removal of either platinum oxide or chemisorbed oxygen by exposure to hydrogen gas with a presumed increasing coverage of the surface by adsorbed hydrogen is seen to slow the rate of return to the zero potential of the normal hydrogen electrode.

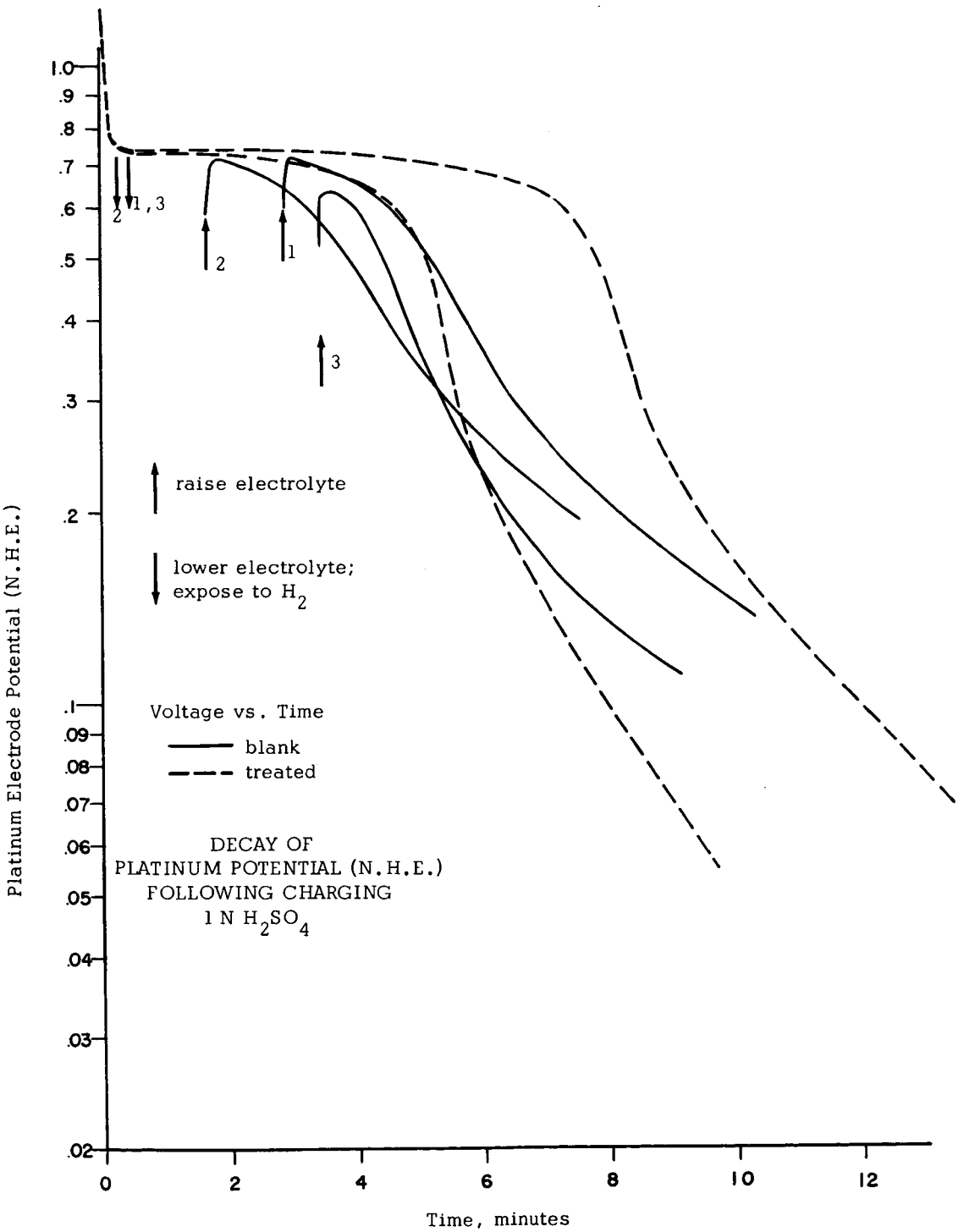
Platinum Electrode Potential (N.H.E.)
1.0
.9
.8
.7
.6
.5
.4
.3
.2
.1
.09
.08
.07
.06
.05
.04
.03
.02
0
2
4
6
8
10
12
Time, minutes
raise electrolyte
lower electrolyte; expose to H_2
Voltage vs. Time
blank
treated
DECAY OF PLATINUM POTENTIAL (N.H.E.) FOLLOWING CHARGING 1 N H_2SO_4
1, 3
2
1
2
3

Figure 1

Concentration Overpotential Transients

Dr. L. Nanis, Mr. A. Adubifa

Mass transfer to or away from the electrode plays an important role in Electrochemistry. Mass transfer processes determine, at a given current density, the concentration changes near the electrode and, therefore, the composition of the solution at the electrode surface which is, in turn, an important factor in electrode kinetics.

This work was undertaken to test a novel method for the determination of local boundary layer thickness in an electrolyte with natural convection prevailing; the method is based on analysis of the transient buildup of concentration polarization following constant current passage. The theoretical treatment has been discussed in a previous report (INDEC-SR-6, 1 July 1965). Briefly, the extreme cases of "no stirring" and "pre-existing stirring" serve to bound real cases and, furthermore, provide a general single result

$$\Phi = \frac{C_{(o,t)} - C_b}{C_{(o,\infty)} - C_b} = \frac{2}{\pi^{1/2}} \chi^{1/2} \qquad \text{Eqn. 1}$$

which is valid in the range $0 < \tau < 0.333$ and where $\tau = Dt/\delta^2$, D = effective diffusion coefficient of ionic species, cm^2/sec, $C_{(o,t)}$ = concentration, mol/cm^3, of ionic species at the electrode at time t, seconds, C_b = bulk concentration, mol/cm^3, of the solution, and δ is the thickness of the boundary layer based on the gradient of concentration at the electrode-electrolyte interface and is one-half of the "true" boundary layer thickness based on a second order von-Karman Pohlhausen approximation.

Apparatus

The apparatus consisted essentially of an electrolytic cell for silver dissolution and auxiliary equipment for measurement of total current and the anode potential relative to a probe reference electrode in the same cell. Figure 1 is a schematic diagram of the apparatus.

The cell was a rectangular glass container, 10.3 cm long, 5.6 cm wide, and 14.4 cm deep. The anode and cathode located at opposite ends were pure silver pieces, 0.02 inches thick, which were trimmed and mounted to fit the sides of the container exactly to insure uniform current distribution. (Each electrode was changed after it had been abraded or plated upon sufficiently to cause variation in current distribution.)

As a reference electrode, a piece of thin silver wire, 0.03 in diameter, shielded by a thin glass capillary tubing, was immersed in the solution with its tip lying at a carefully measured horizontal distance from the vertical anode plate.

Potentials between the anode and the reference electrode (referred to as anodic overpotential) were measured with a Keithley 610A high-impedance electrometer and recorded with a Varian variable-speed chart recorder connected to the electrometer output.

Direct current was supplied through a Heath BE-9 battery eliminator and measured by a precision ammeter, model Avometer.

A standard solution of 0.1 M silver nitrate was used and renewed in the cell after each experimental run.

Experimental Procedure

With the silver electrodes in place, the cell was filled to a height

of 12 cm with 0.1 M silver nitrate solution in all cases.

The electrometer and chart recorder were calibrated at the beginning of each experimental run such that the buildup transients traced by the recorder pens utilized the full width of the chart paper. Current was then passed through the solution until the overpotential of the electrode, recorded on the chart paper, remained constant. Each run was repeated as a check of reproducibility.

From the known chart speed and the buildup curves, the polarization η at successive time intervals was obtained.

Analysis of the concentration polarization curves was used to evaluate the actual boundary layer thickness at any point along the length of the electrode. The fraction of ultimately attained concentration difference (in case of the buildup) was expressed as a function of the steady-state polarization, which is given by use of the Nernst equation for a dissolving anode as

$$\Phi = \frac{C_{(o,t)} - C_b}{C_{(o,\infty)} - C_b} = \frac{e^{Z\eta F/RT} - 1}{e^{Z\eta_\infty F/RT} - 1} \qquad \text{Eqn. 2}$$

where η_∞ = ultimately attained polarization, $(t = \infty)$.

Values of the general term in Eqn. 2 were taken from a machine-computed tabulation of the general term as a function of η.

The scaling factor, D/δ^2, for time permits a fit of overpotential time data through the use of Eqn. 2 and Eqn. 1 on the true time scale. The value of δ requires knowledge of the diffusion coefficient. Results for two different current densities and for various positions from the leading edge of the electrode are given in Table 1 together with theoretically calculated values of δ. The agreement may be seen to be excellent except for near to the bottom of the electrode. This is to be expected since the derivation of δ from hydrodynamic principles does not take into account

the effect of the tank bottom on the electrolyte streaming.

TABLE 1

COMPARISON OF δ FROM ANALYSIS OF BUILDUP TRANSIENTS AND THEORY*

y, cm	J = 0.0075 mA/cm^2		J = 0.015 mA/cm^2	
	δ_{Theo} (mm)	$\delta_{Buildup}$ (mm)	δ_{Theo} (mm)	$\delta_{Buildup}$ (mm)
0.5	0.38	0.41	-	-
1	0.44	0.45	0.38	0.45
2	0.50	0.39	0.44	0.51
3	0.55	0.42	0.65	0.41
5	0.61	0.36	0.53	0.52
8	0.57	0.39	0.58	0.36

* C. Wagner [J. Electrochem. Soc., 104 (1957) 129] using the von Karman method derived the following relation for the thickness, δ, of the diffusion layer for the case of uniform current-density distribution at a vertical electrode.

$$\delta = a\left(\frac{Z F \nu D^2 y}{g \alpha J n_A}\right)^{1/5} \qquad \text{Eqn. 3}$$

where Z = Number of electrons involved in the electrode reaction.

ν = Kinematic viscosity of the solution, cm^2/sec.

F = Faraday constant, 96,500 coulombs/gm-equiv.

ρ = Density of solution, gm/cm^3.

D = Diffusion coefficient of ionic species, cm^2/sec.

y = Distance from leading edge of electrolyte, cm.

g = Gravitational acceleration, 981 cm/sec^2.

α = Densification coefficient ($1/\rho \ \partial\rho/\partial c$), cm^3/mol.

J = Current density, Amps/cm^2.

n_A = Transference number of anion.

a = 3.24

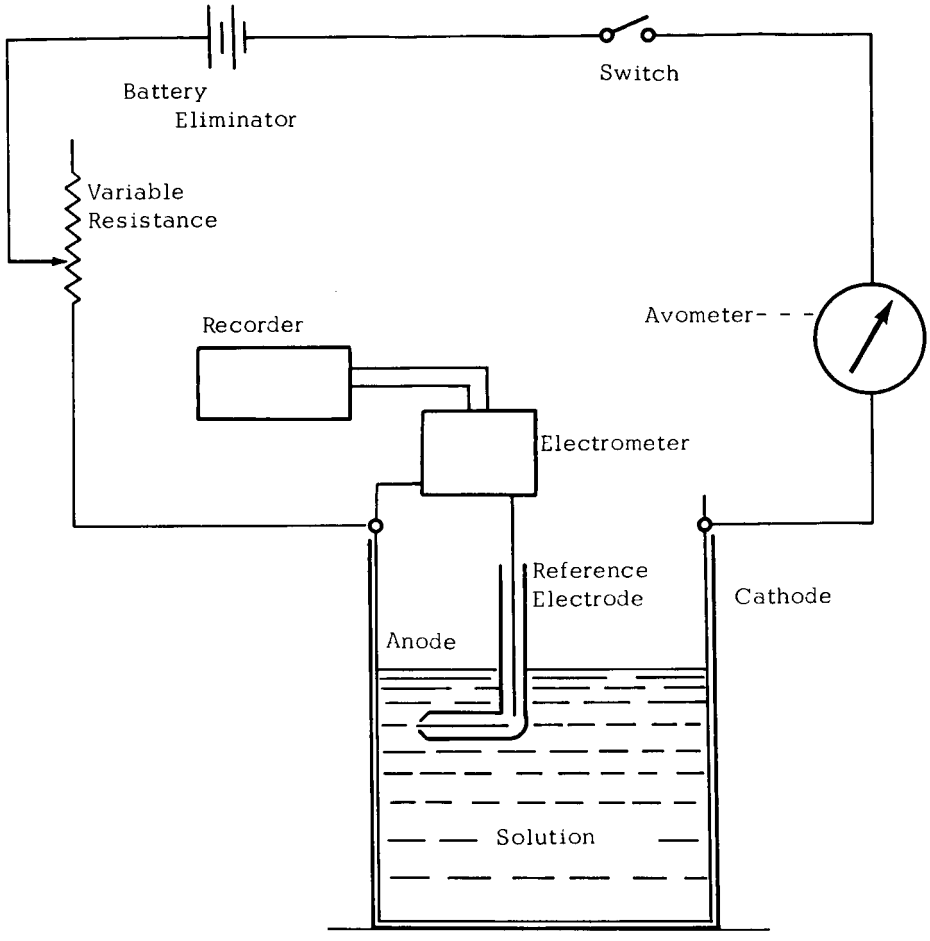
Battery
Eliminator
Switch
Variable
Resistance
Recorder
Avometer
Electrometer
Reference
Electrode
Cathode
Anode
Solution

Figure 1

Galvanostatic Charging Transients

Dr. L. Nanis, Dr. P. Javet

The aim of this study is to find a useful relation describing the time variation of potential, η, following the switching on of a constant current J_T in a galvanic cell. In the absence of mass transport effects, two separate reactions take place:

1. The normal Faradaic reaction, involving current density J_F
2. Charging of the double layer capacity C, using a current density J_c

It is well-known that, for a cathode

$$\frac{J_F}{J_o} = \exp\left(-\frac{\alpha z F}{RT}\eta\right) - \exp\left(\frac{(1-\alpha)zF\eta}{RT}\right) \qquad \text{Eqn. 1}$$

$$J_c = C\frac{d\eta}{dt} \quad \text{(per unit area)} \qquad \text{Eqn. 2}$$

$$J_T = J_F + J_c = \text{total current density} \qquad \text{Eqn. 3}$$

In the most general case, C is a function of η, and the relation between t and η can not be found simply owing to the nonlinear differential equation which arises. Two types of simplification can be made:

1. Let C be independent of the potential. This has been done for a few particular cases by some authors [1,2,3] who have obtained rather complicated mathematical relations, ultimately permitting determination of the relationship between t and η.

2. Approximate the value of J_F, for which two principal approaches are possible, according to the potential range being investigated.

a. Linearization of the exponentials by series expansion, retaining first order terms only, leading to the relation

$$\frac{J_F}{J_o} = \frac{zF}{RT}\eta = b\eta \qquad \text{Eqn. 4}$$

After introduction of the charging current, this equation can be easily integrated (assuming C= constant), with the boundary conditions at $t = 0, \eta = 0$ and at $t = \infty, \eta = \eta_\infty = \text{const}$. Integration of the combination of Eqns. 2, 3, 4 gives the well-known result:

$$\frac{\eta}{\eta_\infty} = 1 - \exp\left(-\frac{t}{bC}\right) \qquad \text{Eqn. 5}$$

However, other ways to approximate Eqn. 1 seem not to have been employed.

b. Tafel approximation is obtained at high overpotentials when the second exponential of Eqn. 1 is negligible. We have in this case for J_T:

$$J_T = J_o \exp\left(-\frac{\alpha Z F \eta}{RT}\right) + C\frac{d\eta}{dt} \qquad \text{Eqn. 6}$$

which can be integrated with one boundary condition: at $t = 0, \eta = 0$

$$t = \frac{C\eta}{J_o} + \frac{CRT}{\alpha Z F J_T} \ln\left[\frac{J_T - J_o}{J_T - J_o \exp\left(-\frac{\alpha Z F \eta}{RT}\right)}\right] \qquad \text{Eqn. 7}$$

But the approximation of Tafel has the drawback that it does not pass through the origin of the η - J coordinates, as does Eqn. 1. It has been proved advantageous to introduce a new approximation in this case, i.e.,

$$J_T = J_o\left[\exp\left(-\frac{\alpha Z F \eta}{RT}\right) - 1\right] + C\frac{d\eta}{dt} \qquad \text{Eqn. 8}$$

which, after integration, leads to

$$t = \frac{C}{J_o + J_T}\eta - \frac{RTC}{\alpha Z F (J_o + J_T)} \cdot \ln\left[1 + \frac{J_o}{J_T}\left(1 - \exp\left[-\frac{\alpha Z F \eta}{RT}\right]\right)\right] \qquad \text{Eqn. 9}$$

The importance of Eqns. 7, 9 is that over a wide range of variation for α, J_o, J_T and C, the real value of t (as it can be computed for low values of the overpotential, η, from Eqn. 5) lies between the values obtained from Eqn. 7 and Eqn. 9. A plot of a typical case is given in Fig. 1.

Such an approach has not been fully exploited or published until now, although the determination of the relation $\eta - t$ is of great interest for the electrochemist.

Further improvements of the calculations, including particularly the most important case where C is not constant, are in progress and are promising.

List of Symbols

Symbol			Units
J_F	=	current density of the Faradaic reaction	Acm^{-2}
J_o	=	exchange current density	Acm^{-2}
α	=	transfer coefficient	dimensionless
Z	=	number of electrons exchanged	$eqt\ mole^{-1}$
η	=	overpotential	mV
F	=	Faraday constant	$A \cdot sec \cdot eqt^{-1}$
R	=	gas constant	$cal\ mole^{-1} degree^{-1}$
T	=	absolute temperature	^oK
J_c	=	charging current density	Acm^{-2}
C	=	capacity of the double layer per unit area	$F \cdot cm^{-2}$
b	=	abbreviation for ZF/RT	
t	=	time	sec

References

1. W. A. Rojter, W. A. Juza, E. S. Polujan Acta Physicochim. URSS, 10 [3] 389 (1939)

2. J. M. Matsen, J. Electrochem. Soc., 110, 222 (1963)

3. L. Karasyk, R. W. Law, H. B. Linford, J. Electrochem. Soc., 111, 237 (1964)

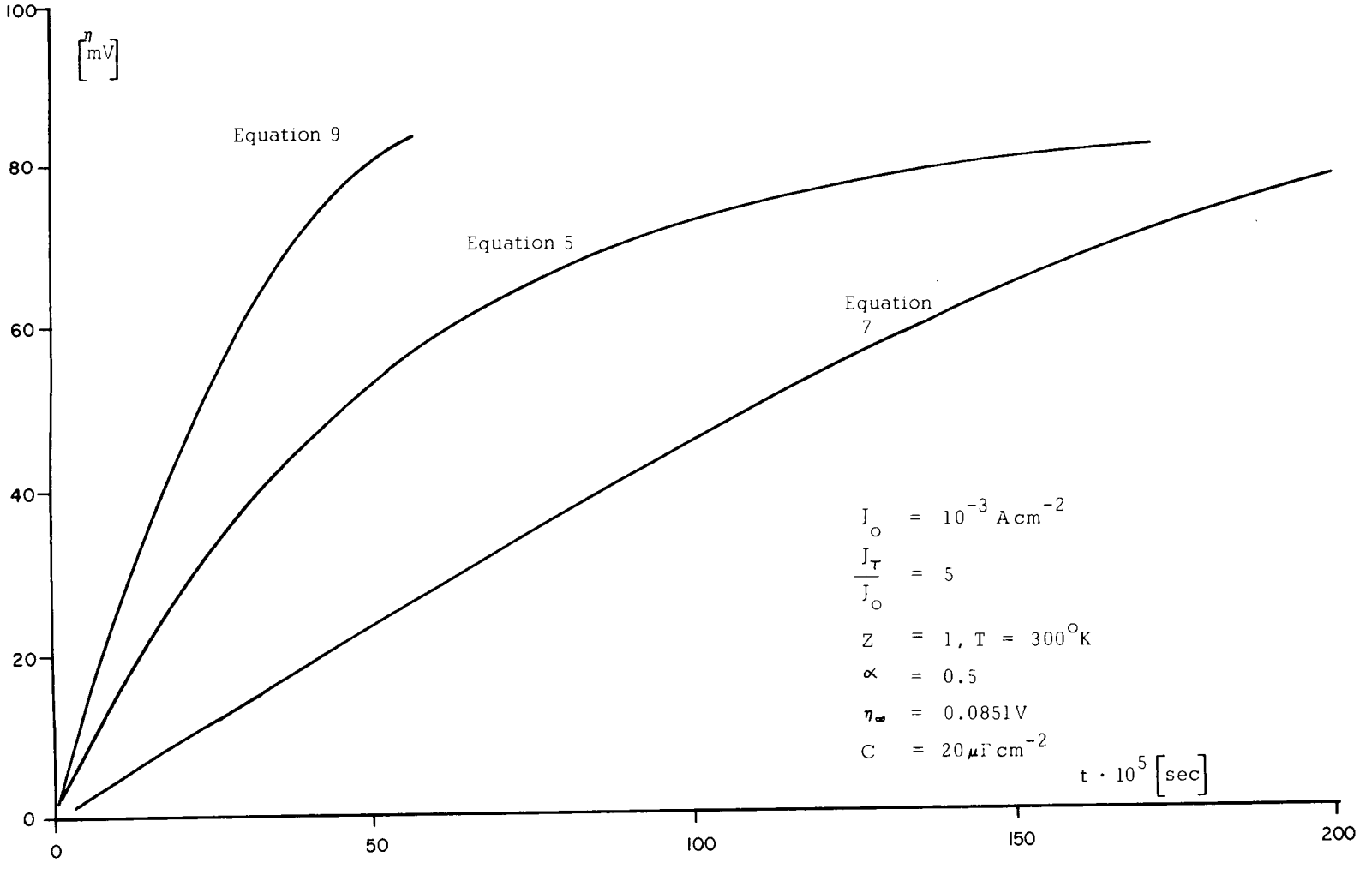

Figure 1

NASA-Langley, 1967 — 23 CR-62039